

#### INTERDISCIPLINARY DOCTORAL SCHOOL

Faculty of Civil Engineering

Eng. Constantin CERNEAGĂ

# NUMERICAL TERRAIN MODELING FOR FLOOD CONTROL IN THE NORTHERN DOBROGEA AREA

# **SUMMARY**

Scientific supervisor

Prof.habil.PhD.Eng.Carmen Elena MAFTEI

BRASOV, 2025

# Cuprins

	•	rag teză
CHAPT	ER I INTRODUCTION	5 <u>16</u>
Conte	KT	5 16
	CATION OF THE TOPIC	
	IVES	
	Content	
CHAPT		
2.1.	FLOOD RISK MANAGEMENT IN EUROPE	9 25
2.2.	FLOOD RISK MANAGEMENT IN ROMANIA	
2.2.2	Legislative and Institutional Framewor	
2.2.2	FRMP – CYCLE I of the Implementation of the Floods Directive	1028
2.2.3	FRMP – CYCLE II of the Implementation of the Floods Directive	11 <u>31</u>
CHAPT	ER III MATERIALS AND RESEARCH METHODS	13_41
3.1. Proba	METHODS FOR CALCULATING DISCHARGES FOR DIFFERENT EXCEEDANCE	13_42
3.1.1	Frequency analysis	13 42
3.1.2	Regional analysis	14 <u>53</u>
3.1.3	Hydrological modeling	14_ <u>53</u>
3.2.	DIGITAL TERRAIN MODEL (DTM)	14 <u>55</u>
3.3.	Flood Hazard Maps	15 <u>61</u>
3.4.	Proposed Methodology	17 <u>70</u>
CHAPT	ER IV CHARACTERIZATION OF THE STUDY AREA	19 72
4.1.	GENERAL OVERVIEW OF THE DOBROGEA REGION	19 <u>72</u>
4.2.	Casimcea Hydrografic Basin	23_80
CHAPT	ER V DEVELOPMENT OF THE DIGITAL TERRAIN MODEL	28_89
5.1.	Terrestrial Measurements	28_89
5.1.1	Equipment Used and Operating Method	29 <u>89</u>
5.2.	PROCESSING AND REPRESENTATION OF THE DIGITAL TERRAIN MODEL (DTM	м) 31 <u>96</u>
CHAPT	ER VI FLOOD MODELING WITH HEC-RAS	33 103
6.1.	MATHEMATICAL MODELING WITH HEC-RAS	33 103
6.2.	ONE-DIMENSIONAL MODELING (1D)	

6.3. Two-Dimensional (2D) Modeling	36 <u>109</u>
CHAPTER VII RESULTS	40 113
7.1. RESULTS OF FLOOD FREQUENCY ANALYSIS	40 <u>113</u>
7.1.2. Analysis of Annual Peak Discharges	40 <u>113</u>
7.1.2. Results of the Frequency Analysis	41 <u>114</u>
7.2. RESULTS OF 1D MODELING	49 <u>125</u>
7.3. RESULTS OF 2D MODELING	52 <u>131</u>
CONCLUSIONS, PERSONAL CONTRIBUTIONS, AND FUTURE PERSPECTIVES	55 <u>135</u>
Research Findings	55 <u>135</u>
Personal Contributions	56 <u>140</u>
Future Perspectives	57 <u>142</u>
SELECTED BIBLIOGRAPHY	58 <u>150</u>

#### Acknowledgements

First and foremost, I wish to express my deepest gratitude to my PhD supervisor, Professor Habil. PhD. Eng. Carmen Elena MAFTEI, for her valuable guidance, constant support, and trust throughout my doctoral journey. Her professionalism, scientific rigor, and openness have played a crucial role in shaping my development as a researcher.

I also extend my sincere thanks to the members of the Advisory and Academic Integrity Board for their insightful observations, constructive suggestions, and support in the development of this thesis. I truly appreciate their involvement and the time they dedicated, which significantly contributed to clarifying and deepening the research topic.

I am grateful to the faculty members of the Faculty of Civil Engineering at "Ovidius" University of Constanța for my academic training and for their support throughout my years of study. In particular, I wish to thank Professor PhD. Eng. Constantin BUTA for his generosity in sharing his knowledge and for his constant encouragement.

Special thanks are due to my colleagues at the Dobrogea-Littoral Water Basin Administration for their professional collaboration, logistical support, and willingness to provide the data necessary for this work.

I am profoundly grateful to my family for their patience, understanding, and unconditional encouragement. Their moral support was fundamental in overcoming all the challenges encountered during this stage of my life.

I dedicate this work, with respect and gratitude, to all those who believed in me, encouraged me, and stood by my side in difficult times. Every contribution, no matter how small, played an important role in the completion of this project, which is so dear to my heart.

# <u>CHAPTER I</u> INTRODUCTION

#### Context

Floods are among the most destructive natural phenomena, with a high potential to cause significant damage. They constitute a destructive natural event [84], not only through the loss of human lives and associated economic damages but also through their substantial impact on the environment, manifested by the alteration of riverbed morphology (both minor and major channels) and the reconfiguration of microrelief in affected regions [106]. In the current context of climate change and the intensification of anthropogenic interventions on the environment [85], both their frequency and extent are increasing.

The term "flood" is defined in Directive 2007/60/EC on the "assessment and management of flood risks" (FRD) as: "the temporary covering with water of land not normally covered by water. This includes floods caused by rivers, mountain torrents, Mediterranean-type ephemeral watercourses, and floods from the sea in coastal areas, but does not include floods from sewerage systems" [87]. This term also covers lowland areas [106] which, due to the rise of the groundwater table until it reaches the surface, become temporarily flooded, resulting in prolonged water stagnation at the soil surface.

The impact of floods is most commonly assessed in economic, social, and ecological terms.

#### România - A Flood-Prone Country

Romania is among the European countries most vulnerable to flood-related risks. The most devastating flood recorded in Romania since 1900 occurred in 1926 [92], resulting in approximately 1,000 deaths. Furthermore, the period between 1960 and 2010 was marked by a high frequency of extreme hydrological events, with over 400 major floods reported [59]. Among the most significant episodes are the floods of May 1970 (215 deaths), July 1975 (60 deaths), July 1991 (108 deaths), and August 2005 (33 deaths) [29], each significantly highlighting the country's hydrological vulnerability.

According to a national risk assessment conducted in Romania [59], floods are among the most destructive types of hazards, characterized by a medium impact on physical, economic, and socio-psychological components, as well as a medium frequency of occurrence.

Amid climate change [16], an increase in flood frequency is projected in numerous river basins, particularly during winter and spring seasons. However, projections regarding the frequency and magnitude of these extreme events remain subject to a degree of uncertainty.

Additionally, within the Danube Basin, Romania has been identified as the country most exposed to the impacts of these climate changes [14].

The Dobrogea-Littoral region is very poor in surface water resources, with the most significant water quantities originating from precipitation. Combined with the relatively low soil permeability, this leads to substantial surface runoff, resulting in frequent flooding.

The areas most affected by historical floods within the Dobrogea-Littoral hydrographic space are the Topolog, Taiţa, and Cartal rivers (the latter being a tributary of the Casimcea River). For the period 2010–2016, the Flood Risk Management Plan (FRMP) – Cycle II [116] also presents the main damages caused by floods in the Dobrogea-Littoral hydrographic area, categorized by consequences, as illustrated in **Fig. 1**.

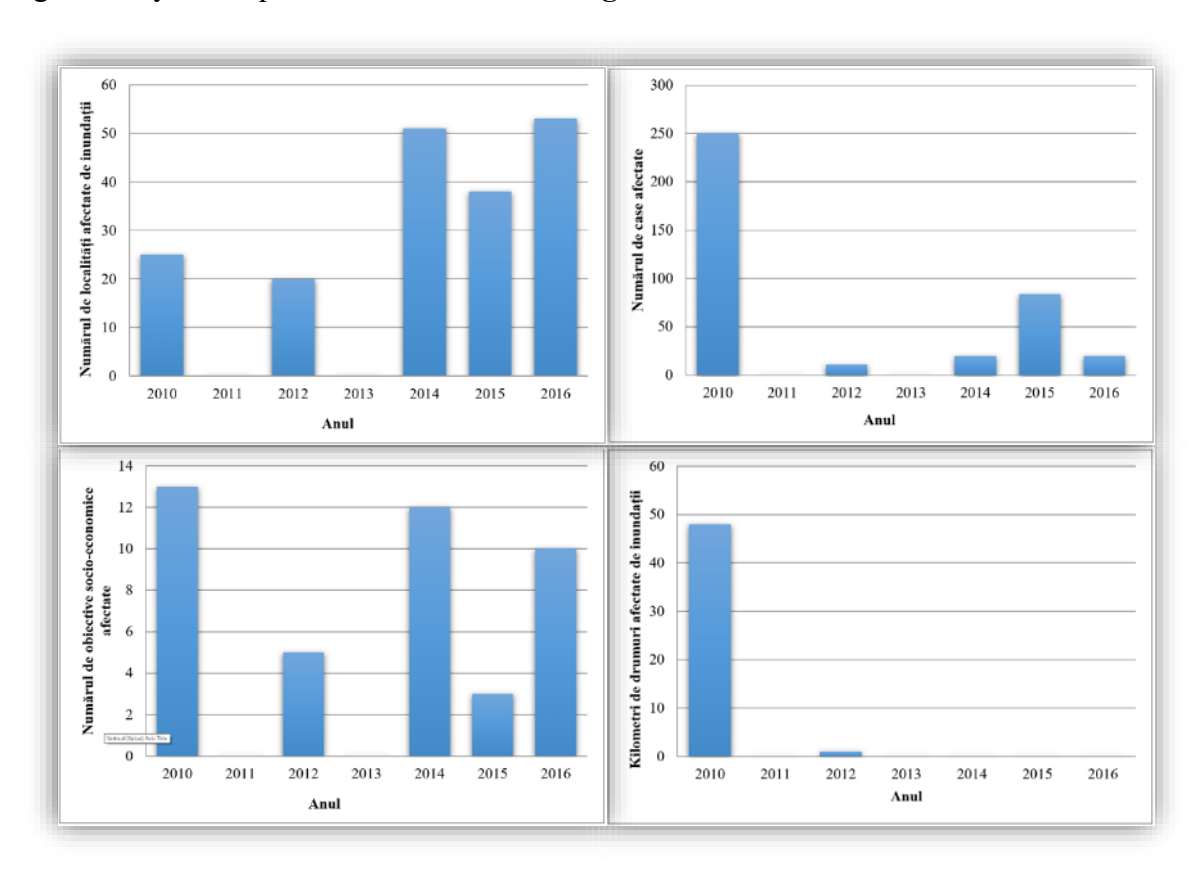


Fig. 1 Flood Damage in the Dobrogea-Littoral Hydrographic Area During 2010–2016 [116]

# Justification of the Topic

The proposed topic is highly relevant in the context of the growing need to improve flood hazard assessment in vulnerable areas, with an emphasis on using modern spatial analysis and hydraulic modeling methods. The localities of Nistorești and Războieni, located in the Casimcea River Basin, are flood-prone zones where the geomorphological and climatic characteristics of the region amplify the potential for such extreme events.

Despite the importance of these areas, current cartographic products regarding flood hazard are either insufficiently detailed or technologically outdated. In this regard, the use of a high-resolution Digital Terrain Model (DTM) – obtained through modern techniques such as LiDAR (Light Detection and Ranging) – and its integration into one-dimensional (1D) and two-dimensional (2D) hydraulic simulation processes contribute to the development of accurate maps that are highly valuable for decision-makers and authorities involved in risk management.

This study aligns with current strategic directions on climate change adaptation and disaster resilience strengthening, addressing European requirements for updating and improving Flood

Hazard and Risk Maps (FHRM). The results provide a robust foundation for concrete prevention, planning, and emergency response actions, as well as a methodological model that can be replicated in other basins with similar characteristics.

Through its technical and scientific approach, the topic advances knowledge in applied hydrology and underscores the importance of integrating detailed topographic data with simulated hydraulic processes to protect communities and infrastructure exposed to flood risk.

## **Objectives**

#### **General Objective**

The aim of this study is to determine the flood-prone areas for the localities of Nistorești and Războieni, located in the Casimcea River Basin, through hydraulic modeling based on a high-resolution digital terrain model. The results are analyzed in comparison with the existing flood hazard maps within the Flood Risk Management Plan (FRMP) for the Dobrogea-Littoral hydrographic area, to assess their degree of alignment and complementarity.

#### **Specific Objectives**

Analyze the role and relevance of using a high-resolution Digital Terrain Model (LiDAR) in hydraulic simulations for the study areas;

Generate flood hazard maps for the analyzed sectors using 1D and 2D modeling;

Identify potential discrepancies between the obtained results and the existing official data to support recommendations for prevention and intervention measures in the event of similar hydrological events.

#### Thesis Content

This thesis is structured into seven chapters, each addressing essential aspects necessary for achieving the general and specific objectives of the research:

- **Chapter I** provides a general theoretical framework on floods. It presents the types of floods and an analysis of major hydrological events in recent decades at the European, national, and local levels, with a focus on the study areas.
- **Chapter II** details the concept of flood risk management, emphasizing the European and national legislative frameworks, and describes the process of developing and implementing Flood Risk Management Plans in Romania.
- **Chapter III** reviews the research methods and the data required for the study. It includes frequency analysis methods for determining discharges with different exceedance probabilities, essential for flood mapping, and presents the proposed methodology.
- **Chapter IV** analyzes the geomorphological characteristics of the Dobrogea-Littoral hydrographic area and provides a detailed description of the Casimcea River Basin,

- including available data from hydrometric stations on the Casimcea River and its tributaries.
- Chapter V outlines the field survey stages conducted in the study areas to obtain high-accuracy digital terrain models. Activities included aerial surveys and ground measurements, followed by data processing and validation. The resulting models accurately represent terrain morphology and form the basis for subsequent hydrological analyses.
- **Chapter VI** focuses on one-dimensional and two-dimensional hydraulic modeling using the HEC-RAS software. It describes the steps of geometry construction, boundary condition definition, and configuration of parameters for steady and unsteady flow simulations.
- Chapter VII presents the results of the frequency analysis applied to the data series, along with delineation of areas potentially affected by floods under similar hydrological events. It concludes with the general findings of the research, personal contributions, and possible future development directions.

# CHAPTER II FLOOD RISK MANAGEMENT

Flood risk management is a complex and integrated process consisting of a set of measures and actions aimed at preventing, mitigating, and managing the negative effects of floods on the population, infrastructure, and natural environment. Its primary goal is to protect human life, preserve heritage, and ensure sustainable development in vulnerable areas.

## 2.1. Flood Risk Management in Europe

Floods are among the most frequent and costly natural disasters affecting Europe, generating significant consequences for the population, infrastructure, and economy. In this context, efficient flood risk management is essential to protect vulnerable communities and reduce the socio-economic impact of these phenomena.

The European Union (EU) has adopted a series of legislative and strategic measures to support member states in their prevention and adaptation efforts. A key example is Directive 2007/60/EC on the assessment and management of flood risks (FRD), which mandates the development of Flood Hazard and Risk Maps (FHRM) as well as Flood Risk Management Plans (FRMP) for each river basin [03]. Additionally, the EU Strategy on Climate Change Adaptation emphasizes improving the resilience of infrastructure and flood protection systems [04].

# 2.2. Flood Risk Management in Romania

Flood risk management in Romania is a complex and essential process for protecting human life, the environment, cultural heritage, and economic activities. It involves implementing a series of measures and strategies aimed at both preventing flood events and mitigating their negative impacts on communities and infrastructure.

#### 2.2.2. Legislative and Institutional Framewor

Romania's accession to the EU required aligning its national water resource management policies with medium- and long-term European strategies and regulations. In this context, to complement the provisions of the Water Framework Directive (2000/60/EC), Directive 2007/60/EC, known as the Floods Directive, was adopted in 2007. This directive obliges member states to assess and map flood hazards and risks and to develop and implement Flood Risk Management Plans (FRMP) to reduce their impacts on the population, environment, and heritage.

The implementation instrument of the Floods Directive, the FRMP, requires three key stages:

- (i) Preliminary Flood Risk Assessment (PFRA);
- (ii) Development of Flood Hazard and Risk Maps (FHRM);
- (iii) Preparation of Flood Risk Management Plans (FRMP) (Fig. 2).

This process is cyclical, with each stage being reassessed, updated, and completed every six years.

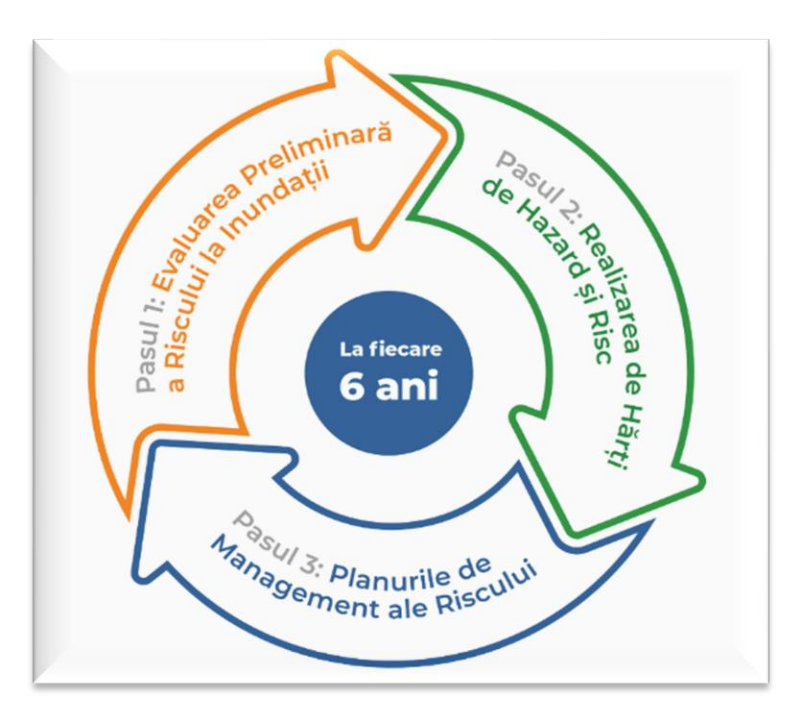


Fig. 2 Stages of the Floods Directive Implementation Process [110]

As an EU member state, Romania transposed this directive into national legislation through Emergency Ordinance no. 3/2010, which amends and supplements the Water Law no. 107/1996, as well as through Government Decision no. 846/2010, which approved the National Flood Risk Management Strategy (NFRMS) for the medium and long term. This strategy was recently updated by Government Decision no. 1566/2024, reflecting the continuous adaptation of national policies to the evolving requirements in flood risk management.

#### 2.2.2. FRMP – CYCLE I of the Implementation of the Floods Directive

- **A.** According to Article 4 of the Floods Directive, the Preliminary Flood Risk Assessment (PFRA) requires member states to conduct an initial analysis including a description of significant historical flood events and the identification of areas with potential significant flood risk. This assessment must address both the hazard perspective (evaluating flood frequency and severity) and its impact, by assessing damages and consequences on the population, infrastructure, and the environment.
- **B.** Flood Hazard and Risk Maps (FHRM) were developed in Romania for areas identified as having significant potential flood risk during the first PFRA stage of the directive's implementation.
- C. Under the directive's requirements, by December 22, 2015, all member states were required to prepare Flood Risk Management Plans (FRMP) (with reporting to the European Commission by March 22, 2016) for all Areas of Potential Significant Flood Risk (APSFRs) identified under Article 5 of the directive and reported to the EC in March 2012. For these areas, the corresponding FHRMs were prepared and transmitted to the EC in March 2014, in accordance with Article 6.

#### 2.2.3. FRMP – CYCLE II of the Implementation of the Floods Directive

Romania completed the first implementation cycle of the Floods Directive in 2016, fulfilling all stages required by this European regulation. The process included the PFRA, the preparation of FHRMs, and the adoption of FRMPs for each Water Basin Administration and the Danube River.

The second cycle of the Floods Directive concluded with Government Decision no. 886 of September 20, 2023, approving the updated flood risk management plans for the 11 Water Basin Administrations and the Danube River in Romania, initially established through Government Decision no. 972/2016. Stage 1 was implemented between 2018–2019 and reported to the EC in September 2019, while the remaining two stages followed the timeline presented in **Fig. 3**.



Fig. 3 Timeline for the Implementation of Floods Directive Cycle II [110]

The implementation of the final two stages of Cycle II was carried out using European funds provided to Romania through the Administrative Capacity Operational Program (POCA) 2014–2020, under the "Support for actions to strengthen the capacity of central public authorities and institutions" framework, Specific Objective 1.1, aimed at developing and introducing common systems and standards in public administration to optimize citizen- and business-oriented decision-making processes, in line with SCAP. This was achieved through the project "Strengthening the capacity of the central public authority in the water sector for the implementation of stages 2 and 3 of Cycle II of the Floods Directive – RO-FLOODS" [115].

Unlike Cycle I of the Floods Directive, which analyzed historical floods over a longer period with limited data on their negative impacts, Cycle II (2010–2016) benefited from a higher level of documentation. This improvement in data quality enabled a more rigorous and precise analysis of the significant negative impacts of historical floods.

Furthermore, during Cycle II, the RO-FLOODS project developed new methodologies for creating Flood Hazard and Risk Maps (FHRM) in Romania. These methodologies were based on the EC report on FHRM [33], FRMP requirements, the EU audit on the Floods Directive implementation in Romania [37], and European best practices.

In conclusion, the implementation of the EU Flood Risk Management Directive in Romania required not only adapting the institutional and legislative framework but also adopting new approaches for flood hazard assessment and mapping. This transition involved significant challenges, especially regarding the updating of methodologies used for hazard determination and risk mapping.

However, the application of the new methodology was not uniform nationwide. In regions such as Dobrogea, no rivers or river sections were proposed for hydraulic remodeling in Cycle II, despite identified issues such as discontinuities in floodplain boundaries within river-crossed localities and adjacent rural areas.

# CHAPTER III MATERIALS AND RESEARCH METHODS

To achieve the established objectives, this study employed a mixed research methodology that combined quantitative and qualitative methods. This approach was applied to conduct an indepth analysis of flood phenomena in the Casimcea River Basin (BH Casimcea), specifically within the localities of Războieni and Nistorești, as well as to map flood extents in these areas.

Quantitative research provided numerical data and objective statistics, enabling rigorous measurement and analysis of the variables involved. Meanwhile, qualitative research offered an in-depth exploration of perspectives, motivations, and individual or collective experiences. By integrating these two methodological approaches, data triangulation was achieved, thereby enhancing the validity of the conclusions and delivering a more comprehensive and nuanced understanding of the relationships identified within the study.

The data used in this research are organized into two main categories:

- (i) Hydrological data regarding the discharges of the Casimcea River and its tributaries;
- (ii) Topographic data.

Hydrological information, consisting of series of mean and maximum discharges recorded at hydrometric stations, is essential both for characterizing the hydrological regime of the Casimcea River and its tributaries and for determining peak discharges with a 1% exceedance probability required in the hydraulic modeling process.

# 3.1. Methods for Calculating Discharges for Different Exceedance Probabilities

To determine the discharges corresponding to hazard levels required by the Floods Directive, the following three methods may be used [73,74]:

- Frequency analysis
- Regional analysis
- Hydrological modeling

#### 3.1.1. Frequency analysis

Frequency analysis is a statistical prediction method used to interpret past events associated with a given process (hydrological or otherwise) to estimate the probability of future occurrences. Prediction involves defining and applying a frequency model, expressed mathematically through an equation describing the statistical behavior of a random variable via its probability distribution function [79].

The application of frequency analysis generally involves the steps illustrated schematically in **Fig. 4**:

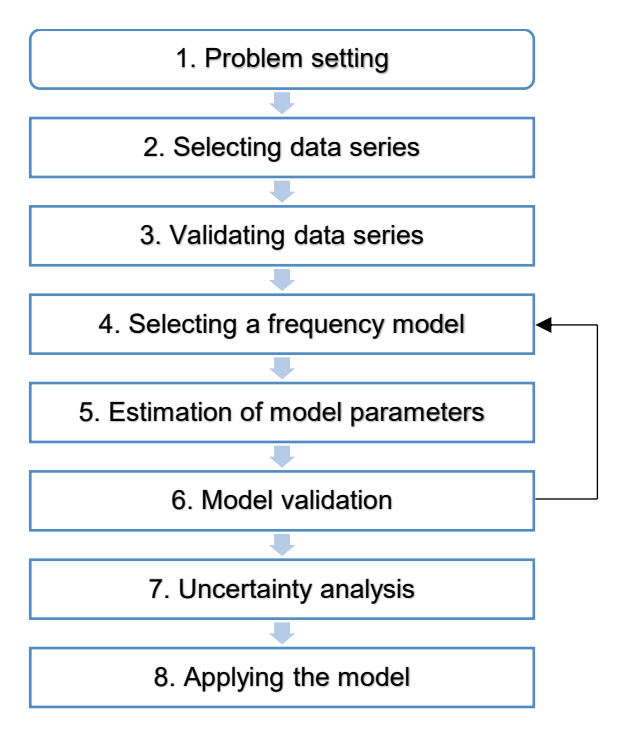


Fig. 4 Stages of Frequency Analysis [78]

#### 3.1.2. Regional analysis

Regional flood frequency analysis is a method used to estimate peak discharges in locations with insufficient hydrometric data by transferring information from hydrologically homogeneous regions. This approach involves identifying regions with similar climatic, morphological, and hydrological characteristics, applying common statistical models, and estimating frequency indicators such as 1%, 2%, or 10% exceedance probability discharges [77].

One of the most commonly applied techniques is the L-moments method, which provides a robust and stable way to derive parameters of extreme value distributions [56]. Within the context of the Floods Directive, regional analysis is recommended where observation records are short or absent, thereby enabling a more coherent estimation of flood hazard.

#### 3.1.3. Hydrological modeling

Hydrological modeling is essential for flood risk assessment because it enables the simulation of surface runoff based on rainfall, basin morphology, soil characteristics, and land cover. This modeling is applied across the entire river basin and involves calculating flood hydrographs for sub-basins, followed by their routing and combination along the hydrographic network.

# 3.2. Digital Terrain Model (DTM)

The term "Digital Terrain Model" (DTM), first introduced by Miller and Laflamme in 1958 [103], was defined as "a statistical representation of the continuous terrain surface using a large number of points with known horizontal coordinates (x, y) and elevation (z), represented within an arbitrary coordinate system."

The representation of terrain relies mainly on elevation, which can reflect relief or other topographic details; hence, the general term "terrain" is used.

When subsurface components (soil structure and geology) are also considered, a more complex three-dimensional representation is obtained, conceptually encompassing the Digital Terrain Model (DTM). However, in practice, as the focus is primarily on the Earth's surface, the appropriate term is Digital Surface Model (DSM).

In geomorphology, the complete term for these digital elevation representations is Digital Elevation Model (DEM). Shorter versions such as DTM or DEM refer specifically to the mathematical approximation of land surface elevation [90].

DTMs are generated through technologies capable of collecting large volumes of spatial data in a short time, such as LiDAR (airborne laser scanning) [61], aerial photogrammetry, sonar, or bathymetric LiDAR in aquatic areas.

The process of creating a DTM generally involves two essential steps:

- Spatial data acquisition
- Digital model construction

# 3.3. Flood Hazard Maps

The development of flood-related maps requires four fundamental components:

- i) Determination of hazard levels,
- ii) Selection of appropriate map scale,
- iii) Application of correct methodologies for discharge estimation for hazard levels,
- iv) Use of flood modeling techniques.

#### A. Flood Hazard

Hazard is a fundamental component of risk, defined as the probability of an event with destructive potential occurring within a specific time frame, affecting people and the environment. From a hydrological perspective, hazard is expressed by the probability of peak discharges being exceeded and includes phenomena like droughts, floods, and related processes such as soil erosion. This study focuses specifically on flood hazard.

In Romania, in accordance with the Floods Directive (FD), three hazard levels are used:

- Frequent events: 10-year return period;
- Medium-probability events: 100-year return period;
- Extreme events: 1000-year return period.

While medium and low-frequency events have long return periods (low probability), their magnitude and potential consequences can be catastrophic. Thus, including such extreme scenarios in hazard mapping is essential.

#### B. Map Scale for Flood Hazard/Risk Maps

The scale of flood hazard and risk maps depends on their intended purpose.

- For public awareness purposes, scales between 1:10,000 and 1:25,000 are recommended, allowing residents to identify risk zones in relation to their homes or workplaces [33].
- For national or regional planning, broader scales such as 1:100,000 to 1:500,000 are used.
- For detailed hydraulic parameter analysis (e.g., water velocity), high-resolution maps at 1:1,000 to 1:5,000 scales are necessary.

According to the EU Flood Mapping Best Practice Guide [42], the choice of scale must align with decision-making levels and information needs, covering four main applications: (1) flood risk management strategy and planning, (2) land-use management, (3) emergency planning and management, and (4) public awareness, including insurance.

#### C. Flood Modeling

Flood modeling is generally performed using hydraulic simulations supported by specialized software. These models allow for the estimation of water levels associated with various hydrological scenarios, forming the basis for delineating flood extents corresponding to different exceedance probabilities.

Mathematical modeling of channel flow, focusing on the processes of flood wave formation and propagation, is a complex but highly valuable approach in the context of integrated water resources management and spatial planning.

Numerical models employ different mathematical formulations depending on the flow regime analyzed. In flood simulations, the most commonly used are models based on the system of equations for unsteady open-channel flow (the Saint-Venant equations) in either 1D or 2D modes.

- 1D Model: In unsteady flow regimes, velocity distribution includes components within the cross-sectional plane, requiring conceptual simplifications in mathematical modeling. These simplifications capture the dominant features of real hydrodynamic processes while omitting secondary influences. The mathematical description of non-uniform unsteady flow in one dimension is based on the Saint-Venant equations.
- 2D Model: Two-dimensional flow modeling is recommended for rivers with wide channels, shallow depths relative to width (B >> h\_B and h\_B >> h), and irregular geometry with significant variations in relief and flow. Under these hydromorphological conditions, depth-averaged velocity components can be introduced for each point within the computational domain. Thus, in 2D modeling, flow velocity is expressed through components u(x,y,t) and v(x,y,t), corresponding to longitudinal and transverse directions, averaged over depth.

In European practice, the most commonly used programs for channel flow modeling are MIKE and HEC-RAS, both providing advanced capabilities for one-dimensional and two-dimensional analyses, thereby enhancing decision-making in flood risk management.

## 3.4. Proposed Methodology

Following a critical analysis of existing methods for determining the topographic and hydrological parameters necessary to develop flood hazard maps, the proposed methodology in this study adopts an integrated approach structured into the following steps:

- [1] Development of a high-resolution DTM, allowing for a detailed representation of terrain morphology essential for accurately mapping flood extents. This DTM addresses limitations identified in hazard maps produced during the first cycle of the Floods Directive (FD) implementation, as outlined in Chapter II
- [2] Estimation of characteristic discharges for various exceedance probabilities (corresponding to specific return periods). Since the analyzed basin is hydrometrically monitored, discharge estimation was performed through frequency analysis, following national flood mapping standards applied under the FD.
- [3] Determination of hydraulic flood parameters—flood extent, water depth, and flow velocity—using numerical simulations in HEC-RAS, conducted in both 1D and 2D for the discharges identified in the previous step.
- [4] Floodplain mapping, achieved by combining hydraulic simulation results (water surface elevations) with the DTM to produce flood hazard maps for the analyzed scenarios.
- [5] Comparison and validation of results with existing hazard maps from the Flood Risk Management Plan (FRMP) for the study areas, highlighting differences and proposing updates to improve these cartographic products.

For the first step, a high-resolution DTM was created by integrating orthophotos, topographic-geodetic surveys, and LiDAR technology. The data were processed using DJI Terra and HEC-RAS software to obtain a detailed terrain morphology representation.

In the second step, hydrological data series for the Casimcea River, including mean and peak discharges, were analyzed. Mean discharges were used to characterize the general hydrological regime, while peak discharges were used to determine exceedance probabilities of 10%, 1%, and 0.1%—relevant thresholds under the FD. Frequency analysis was performed with Hydrognomon software, testing several probability distribution laws to select the best fit for the available data.

To estimate flood parameters (extent, depth, and velocity), hydraulic simulations were conducted in HEC-RAS using its robust hydrodynamic modeling capabilities:

- 1D Modeling: Based on the one-dimensional Saint-Venant equations, involving the definition of cross-sections perpendicular to the river axis where mean water depth and flow velocity are calculated. Between riverbanks and floodplain boundaries, values are interpolated. This model assumes unidirectional flow, generally valid for narrow, well-defined valleys, while lateral flow is neglected. This assumption becomes invalid in wide valleys, low-gradient areas, or deltas where flow distribution is more complex.
- 2D Modeling: Solves the two-dimensional Saint-Venant equations to calculate depthaveraged velocity components in both spatial directions (x and y). This method is better

suited for complex terrains where flow deviates significantly from the main axis, offering a more realistic depiction of flood propagation.

Rationale for using both modeling approaches:

- Floods in Dobrogea typically occur in low-gradient or deltaic areas (e.g., Taiṭa River), often highly urbanized and morphologically complex.
- 2D models provide critical additional information for flood risk assessment, especially for land development planning and infrastructure protection.

Finally, the simulation results deliver a detailed overview of the study areas in relation to historical flood events and are compared against existing FRMP hazard maps to evaluate potential improvements.

# <u>CHAPTER IV</u> CHARACTERIZATION OF THE STUDY AREA

## 4.1. General Overview of the Dobrogea Region

The Dobrogea region, located in southeastern Romania, consists of Tulcea County (in the north) and Constanța County (in the south). Its natural boundaries are well-defined: to the west, the lower course of the Danube River surrounds the Moesian Plateau; to the northwest lie the Casimcea Plateau and the Măcin Mountains; to the northeast, the boundary is marked by the Chilia branch of the Danube Delta; and to the east, it is bordered by the Black Sea coast, which constitutes Romania's seaside boundary.

Overall, Dobrogea is composed of two major distinct morphostructural units that differ in appearance, elevation, formation processes, and geological age:

- The Dobrogea Plateau, on one side,
- The Danube floodplain, the Danube Delta, the coastal plain, and the Razelm-Sinoe lagoon complex, on the other. (**Fig. 5**).

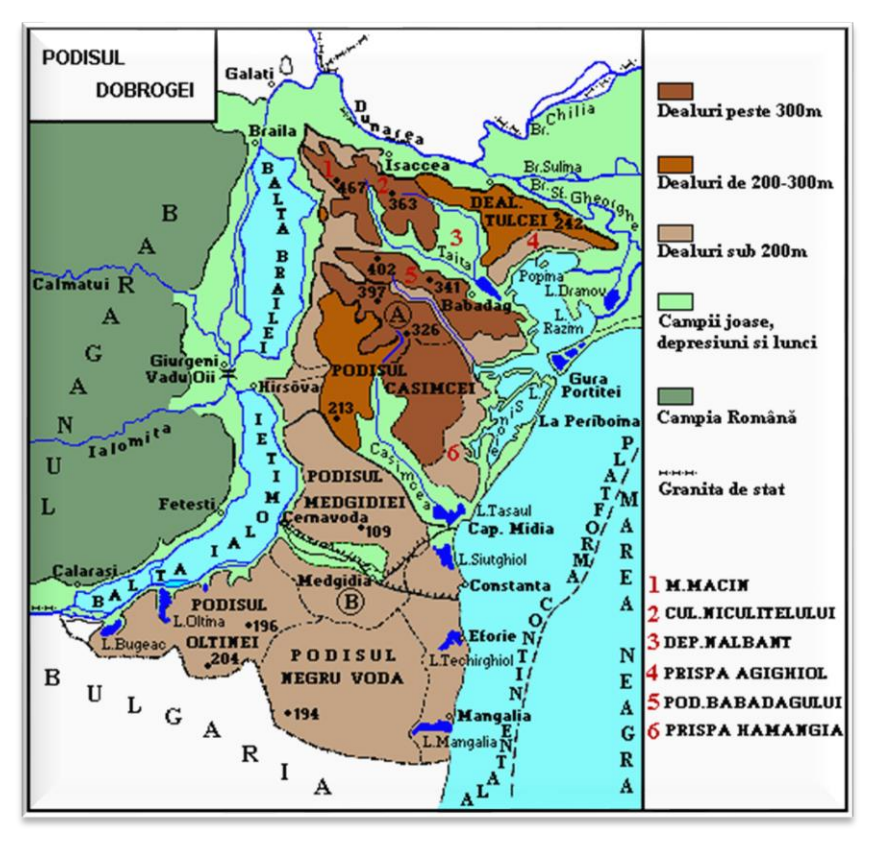


Fig. 5 The Dobrogea Plateau<sup>1</sup>

\_

<sup>&</sup>lt;sup>1</sup> https://www.oocities.org/dmarioara/index.htm

#### Relief

Dobrogea is defined as a relatively rigid plateau composed of ancient rocks (green schists, granites) and Mesozoic and Neozoic sedimentary formations, subjected to prolonged erosion caused by external modeling agents. Its relief is gentle and slightly undulating, with moderate altitudes ranging between 200 and 300 m.

The northern part stands out with higher elevations, locally reaching 350–400 m, and attaining its maximum altitude of 467 m at Pricopan Peak in the Măcin Mountains. In contrast, the southern sector features elevations below 200 m, with a maximum of 204 m in the Deliorman area.

The Central Dobrogea Plateau represents the only and oldest morphostructural unit in Romania, characterized by typical plateau relief, formed from slightly dissected plateaus resulting from advanced erosion, nearing complete leveling (peneplanation) of an orogen that was cratonized as early as the Paleozoic era [01]. Its northern and southern limits are delineated by major deep fault systems: Peceneaga-Camena to the north and Capidava-Ovidiu to the south. (**Fig.** 6) [58].

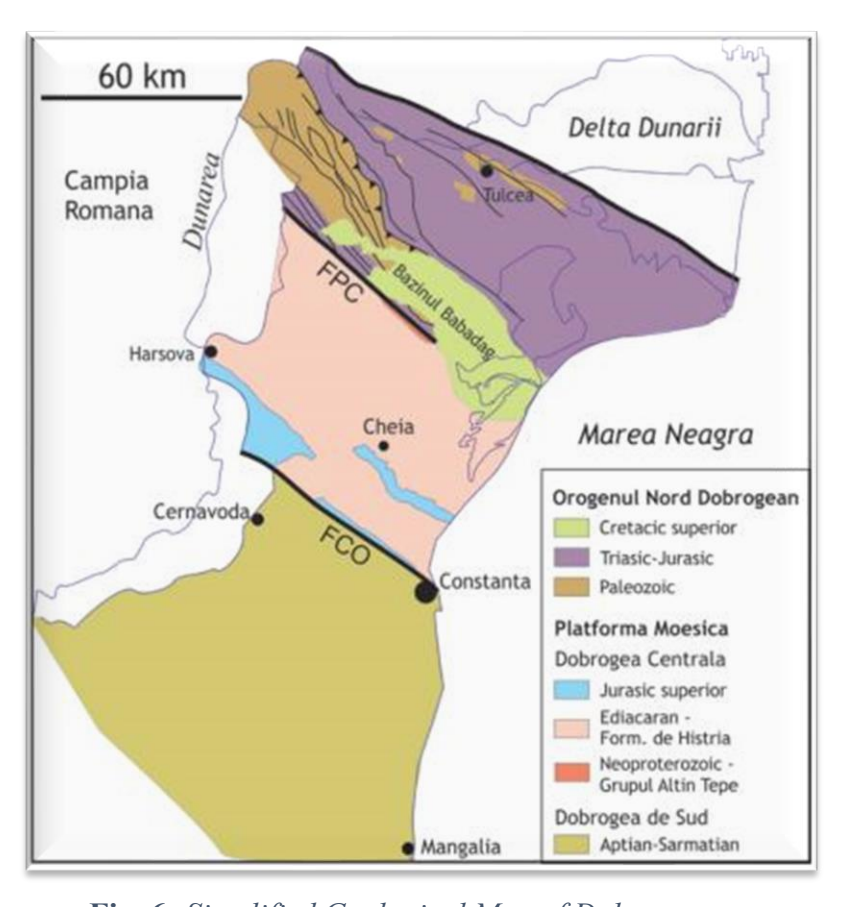


Fig. 6 Simplified Geological Map of Dobrogea [97]

#### Soil

The formation of soils in Dobrogea is directly influenced by relief, parent rock, climate, water resources, and vegetation, which, through their regional characteristics and local manifestations, shape a diverse pedological profile. The region exhibits traits typical of East European steppe zones, leading to a transitional pedogeographic landscape. Loess and loess-like deposits are the most widespread, covering nearly the entire Dobrogea Plateau and providing high

homogeneity of the soil cover from the perspective of parent material, representing a key factor in zonal characterization.

#### Geology

Geomorphologically and evolutionarily, Dobrogea is a complex transitional zone combining ancient landforms such as the Măcin Mountains (remnants of the Hercynian orogeny) with recent landforms created by active alluvial processes, exemplified by the Danube Delta. The region is divided into three major morphostructural blocks:

- Northern Dobrogea characterized by old crystalline formations and Hercynian relics;
- Central Dobrogea dominated by limestone and loess formations with plateau landscapes;
- Southern Dobrogea consisting mainly of low plains, loess deposits, and younger sedimentary layers.

#### Climate

Dobrogea's climate is shaped by continental, sub-Mediterranean, and Black Sea influences, especially along the coastal strip. The region is predominantly arid, with:

- annual average temperatures: 10–11°C,
- summer temperatures: 22–23°C,
- annual precipitation: ~400 mm (among the lowest in Romania),
- frequent droughts and numerous tropical days.

The coastal zone and the Danube Delta are the driest parts of Romania, with annual precipitation rarely exceeding 400 mm. Despite its arid character, Dobrogea exhibits marked rainfall torrentiality, contributing to surface runoff and soil erosion.

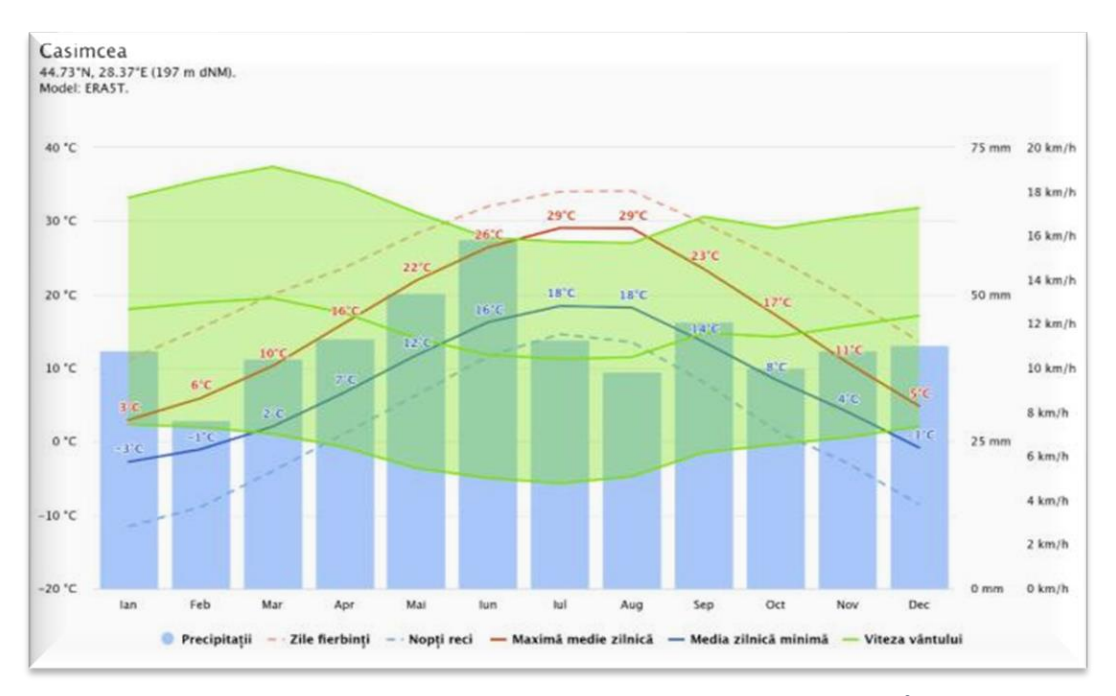


**Fig. 7** *Temperatura și precipitațiile medii - Casimcea*<sup>2</sup>

<sup>&</sup>lt;sup>2</sup> https://www.meteoblue.com/ro/vreme/historyclimate/climatemodelled/casimcea rom%c3%a2nia 682606

In Northern Dobrogea, the wind regime is a key climatic factor, especially affecting the Danube Delta. Winds are particularly intense and frequent during autumn and winter, under the dominance of continental anticyclones, often exceeding 20 m/s. This results in pronounced eolian erosion, microclimatic effects, and significant impacts on river hydrodynamics and adjacent wetlands.

The solid red line represents the average daily maximum temperature, which is the mean value of the highest temperatures recorded in a day for each month of the year, measured at the Casimcea meteorological station. Similarly, the solid blue line indicates the average daily minimum temperature, reflecting the mean of the lowest daily temperatures for each month. Additionally, the dotted red and blue lines highlight the average temperature of the hottest day and the coldest night, respectively, calculated over a 30-year period, thereby emphasizing the monthly averaged extreme values.

#### Hydrography

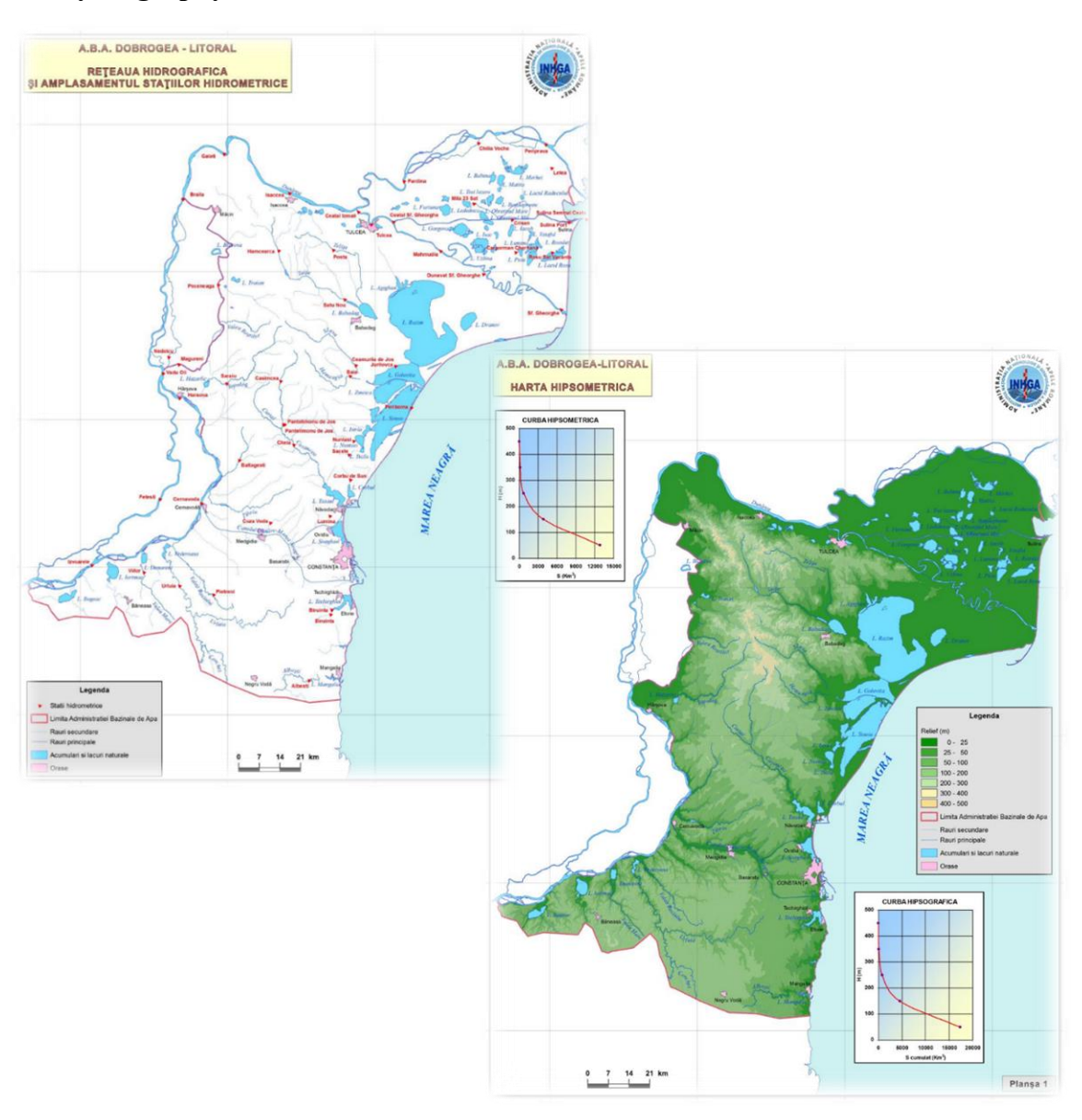


Fig. 8 Rețeaua hidrografică și Harta hipsometrică [114]

The hydrographic network of the Dobrogea-Littoral water basin includes 16 permanent watercourses (**Fig. 8**), with a total combined length of 572 km.

In terms of basin distribution:

- 71% of this length belongs to the Littoral Basin,
- 29% is part of the Danube Basin.

Regionally, 90% of the total river length is located in Northern Dobrogea, while Southern Dobrogea accounts for only 10%, highlighting the uneven distribution of the hydrographic network across the region.

The main inland rivers are: Taiţa and Teliţa, which discharge into Lake Babadag; Slava, which flows into Lake Goloviţa; Casimcea, the most important river in the region, which empties into Lake Taṣaul; and Topolog. In southern Dobrogea, there are intermittent watercourses that flow into the Danube through the fluvial limans located between Ostrov and Cernavodă.

# 4.2. Casimcea Hydrografic Basin

The presentation in this subsection is based on articles [26, 27, 75] published in IOPscience<sup>3</sup>, Springer Nature Link<sup>4</sup> and Hydrology<sup>5</sup>.

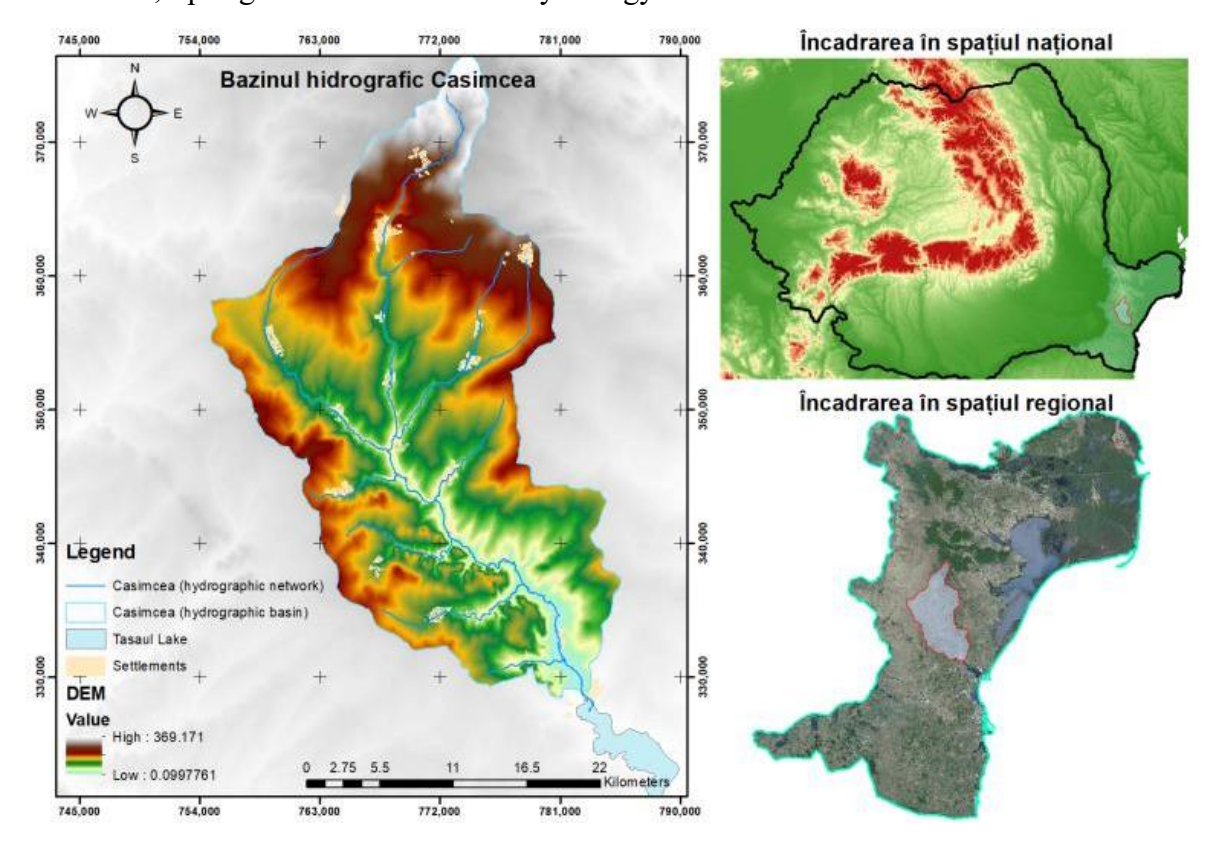


Fig. 9 Location and Representation of the Casimcea Basin [27]

\_

<sup>&</sup>lt;sup>3</sup> https://iopscience.iop.org/article/10.1088/1757-899X/1138/1/012014

<sup>&</sup>lt;sup>4</sup> https://link.springer.com/chapter/10.1007/978-3-030-72543-3 105

<sup>&</sup>lt;sup>5</sup> https://www.mdpi.com/2306-5338/12/7/172

With an area of 740 km² and a main channel length of approximately 69 km, the Casimcea River forms the largest hydrographic basin in Dobrogea (**Fig. 9**). Its relief exhibits a stepped descending arrangement, from the north, where Ciolpan Hill reaches an altitude of 359.2 m, towards the south, near Movila Samen (55 m altitude) [43], and finally to its outlet into Lake Taṣaul. The basin's average altitude is approximately 309 m, with an average terrain slope of around 4%, gradually decreasing toward the discharge area

#### Hydrological Regime of the Casimcea Basin

The Casimcea Basin hosts four hydrometric stations:

Two stations on the main course of the Casimcea River: Casimcea and Cheia;

Two stations on its main tributaries: Pantelimon stations, located on the Cartal and Râmnic streams (**Fig.** 10).

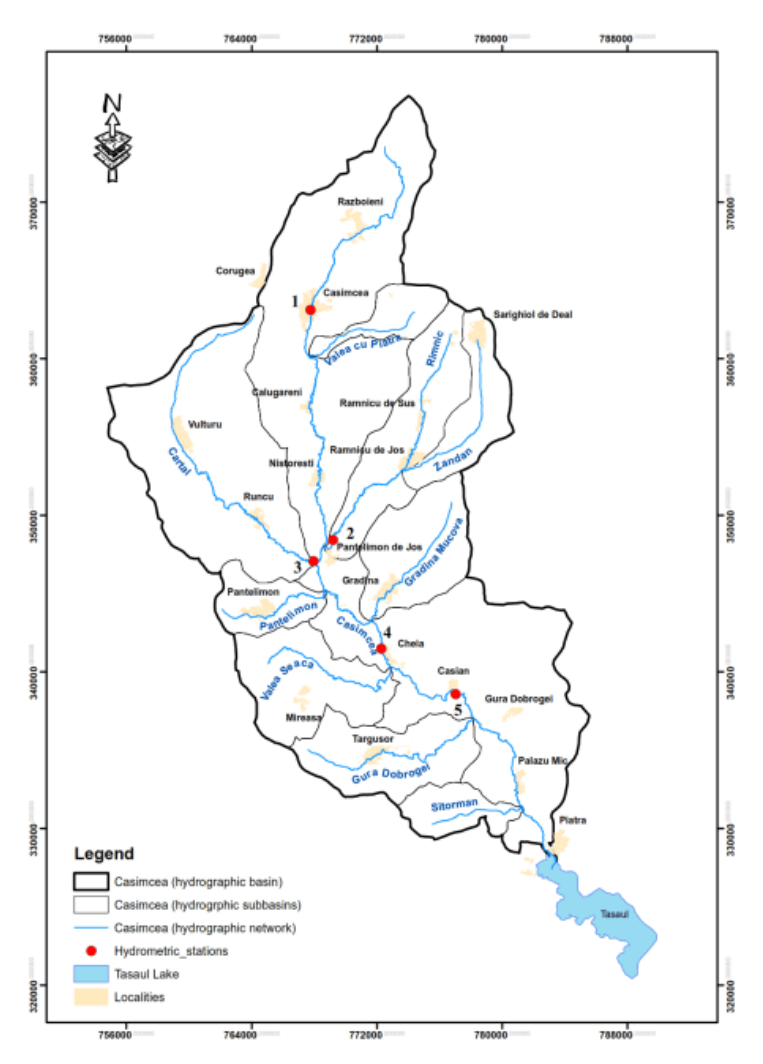


**Fig. 10** *Hydrometric Stations – Casimcea Basin* [75]

To determine the hydrological regime, the time series of mean discharges was used. The analysis relied on the annual mean discharges of the Casimcea River recorded at the following stations: Casimcea, Râmnic, Cartal, and Cheia.

The data, obtained from ABADL, cover the period 1954–2021.

Overall, the annual discharges exhibit low values, with averages ranging between 0.074  $\text{m}^3/\text{s}$  at Râmnic and 0.585  $\text{m}^3/\text{s}$  at Cheia (**Tab.** 1).

**Tab. 1** Descriptive Statistics of the Four Time Series

Statistica	Casimcea	Ramnic	Cartal	Cheia
Mean	0.085	0.074	0.128	0.585
Standard Error	0.005	0.004	0.009	0.034
Median	0.071	0.068	0.115	0.567
Mean Deviation	0.042	0.029	0.070	0.279
Kurtosis	0.846	-0.249	8.566	0.940
Skewness	1.076	0.635	2.113	0.892
Minimum	0.028	0.031	0.000	0.219
Maximum	0.227	0.144	0.461	1.480
No. of records	67	65	56	68

The analysis of statistical data collected from the four hydrometric stations in the Casimcea Basin highlights significant variations in the measured parameters.

- Cheia Station stands out with the highest mean discharge (0.585 m³/s) and maximum value (1.480 m³/s), suggesting a greater intensity of hydrological processes in this area, likely influenced by specific local hydrological and morphological conditions.
- It is followed by Cartal Station with a mean discharge of 0.128 m<sup>3</sup>/s,
- Casimcea Station with 0.085 m<sup>3</sup>/s,
- And Râmnic Station with 0.074 m³/s, both reflecting lower average discharge values.

These differences emphasize the spatial variability of hydrological dynamics within the basin, shaped by catchment characteristics and local geomorphology.

Regarding the hydrological regime, the multi-annual average monthly discharge was determined for all four hydrometric stations.

The Casimcea hydrometric station exhibits a bimodal hydrological regime, with two annual discharge peaks:

- The first peak occurs in February, reaching 0.138 m<sup>3</sup>/s, primarily influenced by snowmelt and early spring precipitation.
- The second peak appears in June, slightly lower at 0.108 m<sup>3</sup>/s, driven mainly by late spring and early summer rainfall.

Following these peaks, discharges decrease below the multi-annual average of 0.085 m³/s, reaching minimum values in September (0.056 m³/s) and November (0.058 m³/s), largely due to high evapotranspiration rates and reduced water inputs during the late summer and autumn periods.

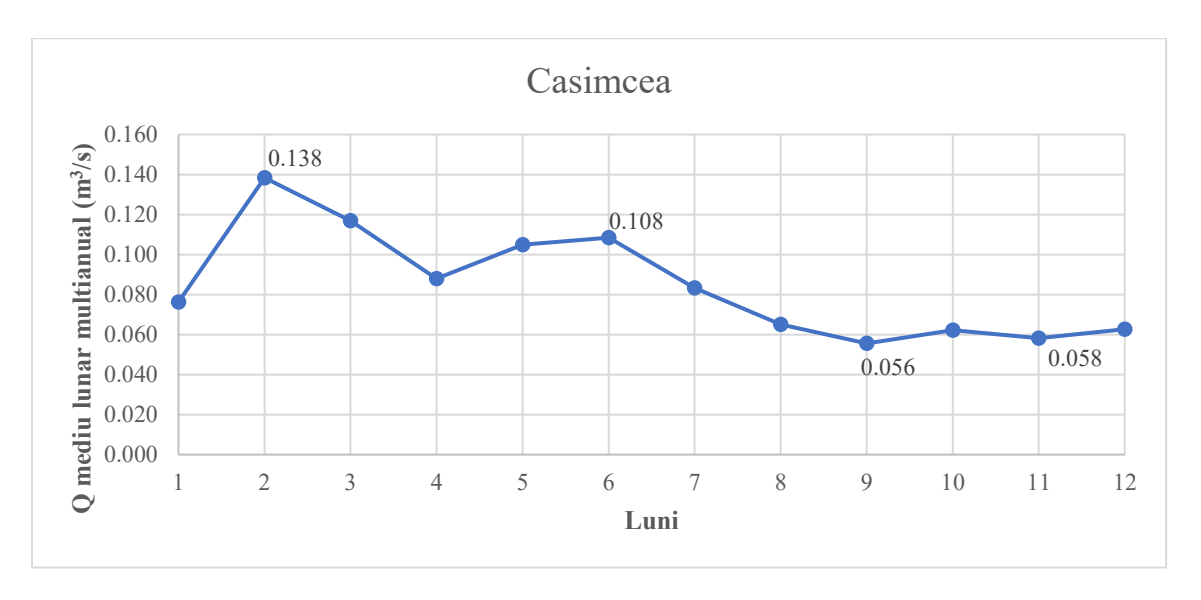


Fig. 11 Multi-annual Monthly Hydrological Regime (1955–2021) – Casimcea Station

The monthly hydrological regime of the Casimcea River and its tributaries is bimodal, with two distinct peaks and two evident low-flow periods throughout the year.

The geological nature of the basin, dominated by limestone formations, facilitates water infiltration into the subsurface, reducing surface runoff and influencing streamflow dynamics. Consequently, both precipitation patterns and lithological characteristics play a key role in shaping discharge variability in the Casimcea Basin.

In the Dobrogea Plateau, where the Casimcea River is located, floods are predominantly localized, typically triggered by single torrential or quasi-torrential flash floods affecting most valleys.

Under heavy rainfall conditions, the hydrological response of the basin is intensified by runoff contributions from its tributaries—Pantelimon, Cartal, Râmnic, and Mucova.

As a result, in the Casimcea locality, floods occurring between 2002–2013 caused significant destruction, including the demolition of houses and farms, as well as damage to schools, churches, agricultural land, and critical infrastructure (roads, bridges, etc.).

Flooding events are most frequent during May–July, underscoring the seasonal nature of these phenomena and their connection to summer atmospheric instability. Extreme daily precipitation values (>70 mm) have been responsible for the most devastating events, confirming the basin's high vulnerability to extreme hydrometeorological phenomena.

The most extreme recent event, which caused the largest flood damages in the Casimcea Basin, occurred on May 30, 2002, recorded at the Casimcea hydrometric station. Based on FRMP Cycle I data, the flood hydrograph for this event is presented in **Fig. 12**:

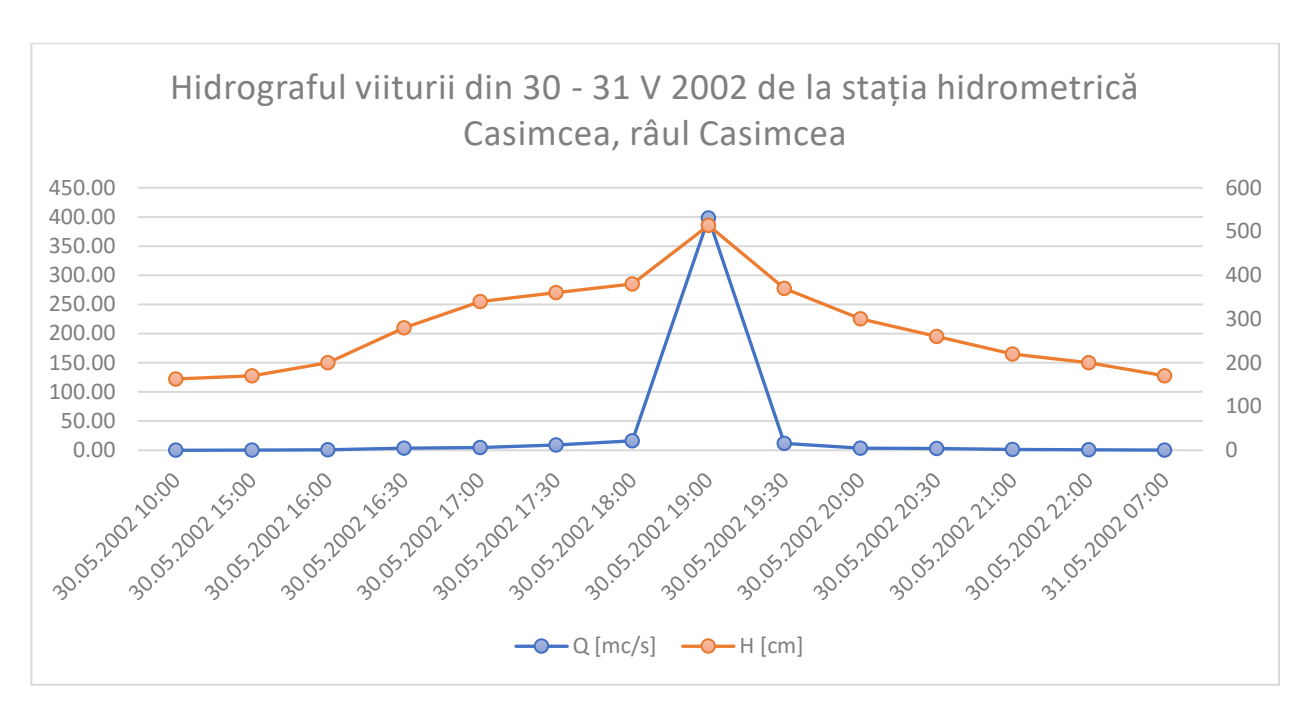


Fig. 12 Flood Hydrograph of May 30–31, 2002, at Casimcea Hydrometric Station [26]

Based on the values recorded between May 30–31, 2002, a clear and rapid evolution of both discharge and water level can be observed, culminating in a peak flow of 398 m<sup>3</sup>/s at 19:00.

The shape of the hydrograph indicates a simple (or singular) flood wave, defined by:

- A single well-marked peak,
- A short rise and fall period.

This configuration suggests a quickly generated flood resulting from a high-intensity event with concentrated temporal rainfall distribution.

The torrential nature of the event is confirmed by the sudden increase in discharge from 0.79 m<sup>3</sup>/s to 398 m<sup>3</sup>/s within only three hours, followed by a rapid decrease to below 4 m<sup>3</sup>/s in the next hour.

These characteristics reflect a short response time, typical of small basins with steep slopes, classifying the event as a flash-flood with a total duration fitting within the rapid flood category.

# CHAPTER V DEVELOPMENT OF THE DIGITAL TERRAIN MODEL (DTM)

The creation of Digital Terrain Models (DTM) involves a complex process of data collection, processing, and analysis using advanced technologies such as GNSS RTK (Real Time Kinematics), LiDAR, aerial photogrammetry, and/or total stations, combined with specialized software tools.

#### 5.1. Terrestrial Measurements

The process begins with measurement planning, where the study area is delineated, objectives are defined, and the appropriate data collection methods are selected. Following this stage, the equipment and measurement parameters are configured to ensure the required accuracy of the collected information.

Data collection was carried out using GNSS RTK measurements (**Fig. 13**), which provide point coordinates with high precision [69]. Additionally, LiDAR technology and aerial photogrammetry were used to generate dense point clouds, resulting in a highly detailed representation of the terrain surface.

The density and accuracy of these points depended largely on the technology employed, the characteristics of the surveyed area, and the parameters established during the planning stage..

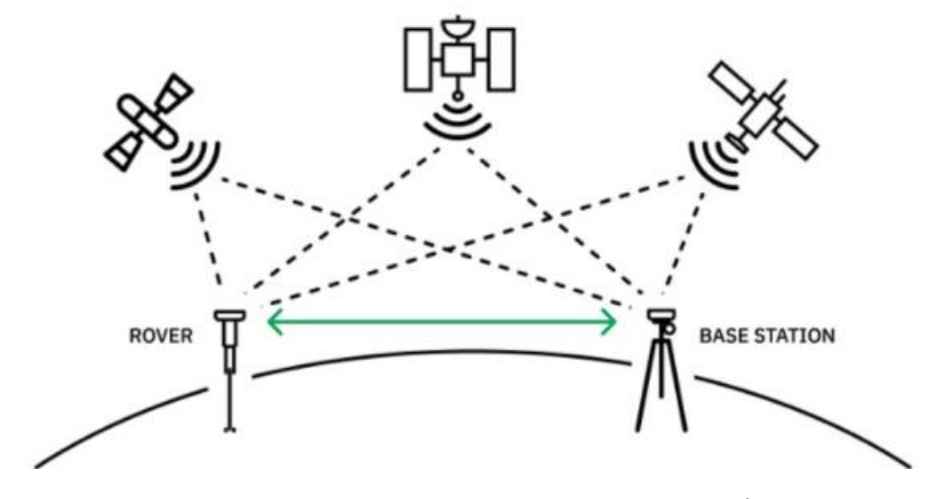


**Fig. 13** Data Transmission in RTK System <sup>6</sup>

.

<sup>&</sup>lt;sup>6</sup> RTK Corrections: What This Means & How It Works – pointonenav.com

#### 5.1.1. Equipment Used and Operating Method

Trimble R780 GNSS Receiver

The Trimble R780 (**Fig. 14** - left) is an advanced GNSS receiver designed to provide high-precision positioning even in challenging environments. It enables highly accurate measurements through RTK (Real-Time Kinematic) technology. In this study, it was used in conjunction with the national network of permanent stations, ROMPOS (Romanian Position Determination System), thus delivering real-time corrected positions with centimeter-level accuracy.

When connected to the TDC 600 controller (**Fig. 14** - right), the receiver gains internet access via mobile data (network – Wi-Fi/SIM card/hotspot), ensuring continuous data transmission and real-time corrections.



Fig. 14 GNSS Trimble R780 Reciver<sup>7</sup> and TDC600 controller<sup>8</sup>

DJI Matrice 350 drone and LiDAR Zenmuse P2 sensor

**DJI Matrice 350 RTK** (**Fig. 15**) is one of the most advanced drones for mapping and surveying, due to its high precision, extended flight autonomy, and compatibility with specialized equipment. It is used for collecting highly accurate geospatial data, making it ideal for producing 2D and 3D maps, digital terrain models (DTMs), and photogrammetric reconstructions.



**Fig. 15** *DJI Matrice 350 RTK Drone with Remote Controller and Included Accessories*<sup>9</sup>

,

<sup>&</sup>lt;sup>7</sup> R780 GNSS Smart Antenna | Trimble Civil Construction

<sup>&</sup>lt;sup>8</sup> Trimble TDC600 | Trimble Utilities

<sup>&</sup>lt;sup>9</sup> DJI Matrice 350 RTK

The drone is remotely operated via the DJI RC Plus controller, equipped with a 17.78 cm high-brightness touchscreen, ensuring optimal visibility under all lighting conditions..

The drone is equipped with RTK technology, which provides centimeter-level positioning accuracy, significantly reducing the need for ground control points.

For each area of interest, predefined flight perimeters are uploaded according to the mission's purpose. To generate the Digital Terrain Models (DTMs), the DJI Zenmuse L2 LiDAR sensor was employed, with flight parameters set to a speed of 10 m/s and an altitude of 70 m above ground level.

The **Zenmuse L2** is a high-precision aerial LiDAR system, integrating:

- A LiDAR unit for accurate surface scanning,
- A high-accuracy internally developed IMU (Inertial Measurement Unit),
- An RGB mapping camera equipped with a 4/3 CMOS (Complementary Metal-Oxide-Semiconductor) sensor.

This configuration enables DJI aerial platforms to acquire more precise, efficient, and reliable geospatial data. When used in conjunction with DJI Terra software, Zenmuse L2 provides a comprehensive solution for high-accuracy 3D data collection and post-processing.



Fig. 16LiDAR Zenmuse L2 sensor<sup>10</sup>

This advanced LiDAR system is ideal for applications such as mapping, surveying, and other fields requiring highly accurate geospatial data acquisition.

The data collected by the sensor, stored in its external memory, include:

- LiDAR files (.LID): Raw point cloud data;
- RTK files (.RTK): GNSS correction data;
- RGB images: Used for point cloud colorization and orthophoto generation.

These files are subsequently downloaded for processing and analysis using specialized software, as described in the following stages.

\_

<sup>&</sup>lt;sup>10</sup> DJI Zenmuse L2 - SkyGrid

#### 5.2. Processing and Representation of the Digital Terrain Model (DTM)

After field data collection, the next step is data processing, which involves:

Correcting errors and inconsistencies;

Filtering raw data to remove noise;

Interpolating the measured points to generate a continuous surface model.

This step relies on specialized software tools such as DJI Terra, Pix4D Mapper, and Global Mapper, which allow efficient generation of high-resolution DTMs and derivative geospatial products.

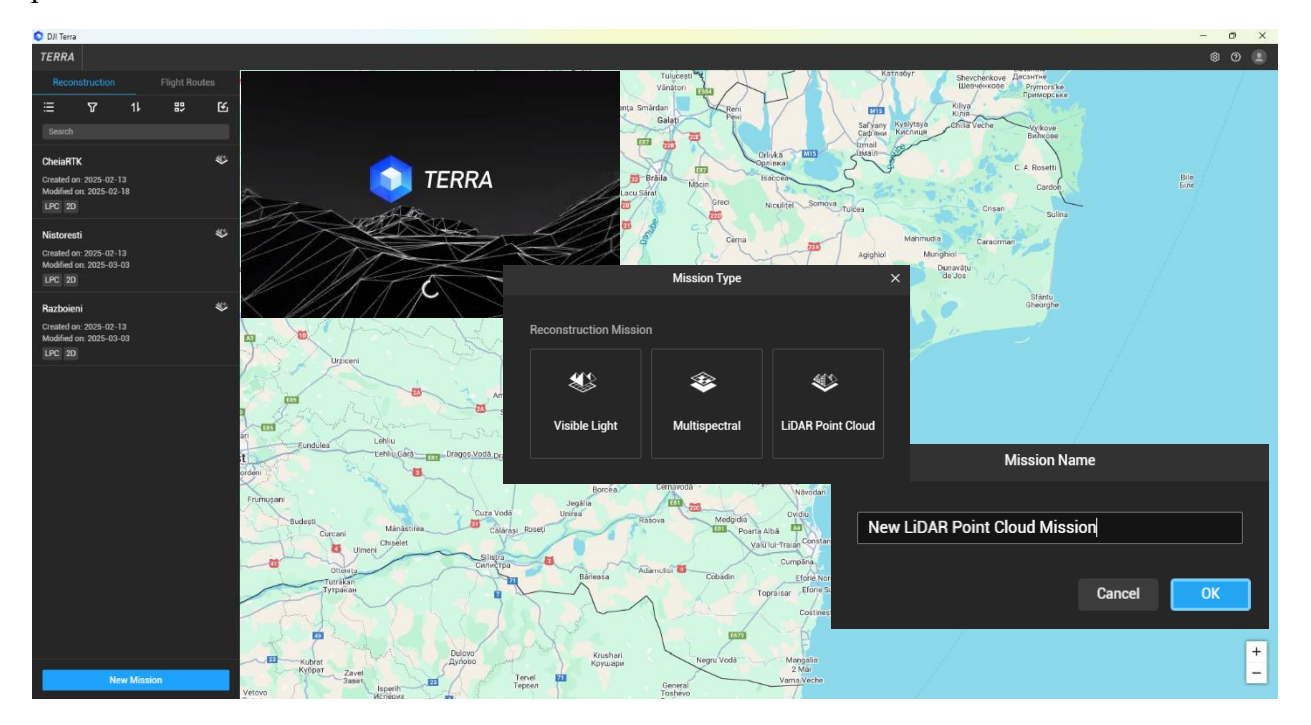


Fig. 17 DJI Terra interface

The data collected using the Matrice 350 RTK drone with the Zenmuse L2 sensor were processed in DJI Terra (Fig. 17).

The outputs generated include both 2D products and 3D high-density LiDAR point clouds, which can subsequently be integrated into GIS applications or hydraulic models for purposes such as spatial analysis, flood simulations, volumetric estimations, and land-use planning.

Given that the resulting model is later employed for flood simulation, the point cloud undergoes a post-processing phase, during which artificial elements (e.g., buildings, vehicles, vegetation) are removed. This step leads to the generation of the Digital Elevation Model (DEM), accurately representing the terrain's morphology and suitable for integration into the proposed hydraulic models.

The software automatically uses the acquired data to generate a quality report at the end of processing. This report includes flight parameters and a statistical accuracy assessment of the

model, compared to the previously defined ground control points (GCPs). Based on this information, the accuracy of the results can be evaluated. A comparative overview of the two quality reports obtained from data processing is presented in the following tables (Error! Reference source not found.):

**Tab. 2** General Information on Flight and Processing

Caracteristică	Războieni	Nistorești
Effective flight time	27 min 21 s	25 min 23 s
Total processing time	5 h 40 min	4 h 25 min
Mapped area	0.485 km <sup>2</sup>	0.504 km <sup>2</sup>
Orthophotomap GSD (TDOM)	2.57 cm/pix	2.09 cm/pix
Average point cloud density	612 puncte/m <sup>2</sup>	584 puncte/m <sup>2</sup>

**Tab. 3** *Altitude Accuracy (validation with GCP)* 

Parameter	Războieni	Nistorești
Average flight altitude	69.6 m	75.6 m
Average flight speed	8.2 m/s	8.61 m/s
Coordinate system	Stereo70	Stereo70
Number of control points	6	6
Mean elevation error (Z)	−0.089 m	−0.107 m
Mean absolute error	0.089 m	0.107 m
Elevation RMSE (Root Mean Square Error)	0.0978 m	0.1181 m
Standard deviation	0.0893 m	0.1181 m
Maximum error	−0.102 m	−0.140 m

Both flights produced high-density and high-precision results, suitable for generating DEMs and orthophotomaps required for hydraulic modeling. The Războieni area, characterized by more rugged terrain, recorded a slightly lower error compared to the Nistorești area, which has a flatter topography. However, the differences are minimal (less than 2 cm), indicating a high degree of accuracy for both datasets.

The final stage of the workflow involves the analysis and utilization of the resulting terrain models. These serve as a crucial basis for topographic assessment and can be applied to various purposes, including:

- Slope calculations,
- Surface runoff modeling,
- Drainage network analysis,
- Identification of potential water accumulation areas.

Additionally, DTMs are valuable for infrastructure projects, urban planning, land-use management, and sustainable natural resource management. A high-precision terrain model enhances decision-making quality and optimizes processes in planning, design, and intervention within both built and natural environments.

# CHAPTER VI FLOOD MODELING WITH HEC-RAS

# 6.1. Mathematical Modeling with HEC-RAS

Mathematical modeling in HEC-RAS involves simulating water flow within river systems or open channels using fundamental hydraulic equations. This software (**Fig. 18**), developed by USACE (U.S. Army Corps of Engineers), enables the creation of 1D and 2D flow models to analyze water behavior under various scenarios [49].

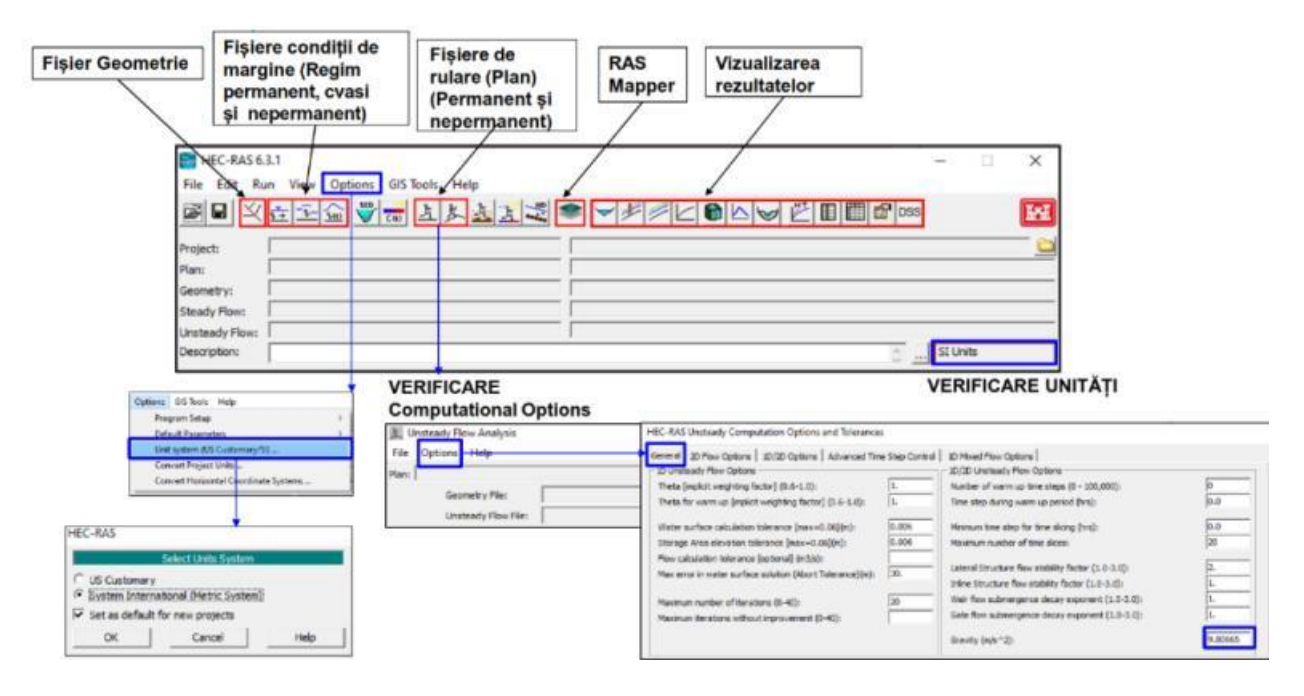


Fig. 18 HEC-RAS Program Interface

RAS Mapper, the integrated graphical module of the HEC-RAS program, is used for both spatial data processing and visualization of results generated through hydraulic modeling. Simply put, it allows the creation, editing, and display of maps and GIS layers associated with modeling, providing an interactive visual interface for configuring and interpreting spatial data.

# 6.2. One-Dimensional Modeling (1D)

1D modeling in HEC-RAS involves simulating water flow in a single plane, along the longitudinal direction of a river or channel, considering flow variations only along the river axis and not accounting for the transverse distribution of hydraulic parameters.

After the initial project setup and the import of the Digital Terrain Model (DTM), the geometry of the 1D model is developed, forming the foundation for hydraulic simulation.

Key steps include:

- Drawing the river centerline (flow path): A polyline representing the main course of the river, defining the flow direction.
- Defining riverbanks and floodplain boundaries: Differentiates between the main channel (active bed) and potential inundation areas.
- Creating cross-sections: Placed perpendicular to the flow axis, either at regular intervals or at key locations (bends, confluences, bridges, etc.).
- Assigning hydraulic parameters: Includes Manning's roughness coefficients, representing resistance to flow in both the channel and floodplain, as well as hydraulic structures (bridges, levees, weirs) that influence flow dynamics.



Fig. 19 RAS Mapper – Geometry 1D

After creating and drawing the basic geometric elements (river centerline, banks, and cross-sections), they are saved and further analyzed in the Geometric Data Editor window in HEC-RAS. At this stage, essential adjustments are made to the cross-sections to accurately reflect the morphological reality of the riverbed.

#### Specifically:

- Modification of the minor channel limits: This involves identifying the positions of the left and right banks, enabling the model to correctly distinguish between the active channel (frequent flow area) and the floodplain (major channel). This delineation significantly impacts the computation of velocity distribution and energy losses.
- Definition of Manning's roughness coefficients (n): For each section, separate values are typically assigned for the minor channel and the floodplain, depending on factors such as substrate type, vegetation cover, the presence of structures, or other obstacles affecting flow resistance.

In the case of 1D modeling, Manning's coefficients were manually assigned based on the morphology of each section, field observations, and satellite imagery analysis. The coefficients were selected in accordance with Chow's (1959) classification for natural streams, taking into account substrate type, bank vegetation, channel sinuosity, and other relevant elements influencing flow resistance.

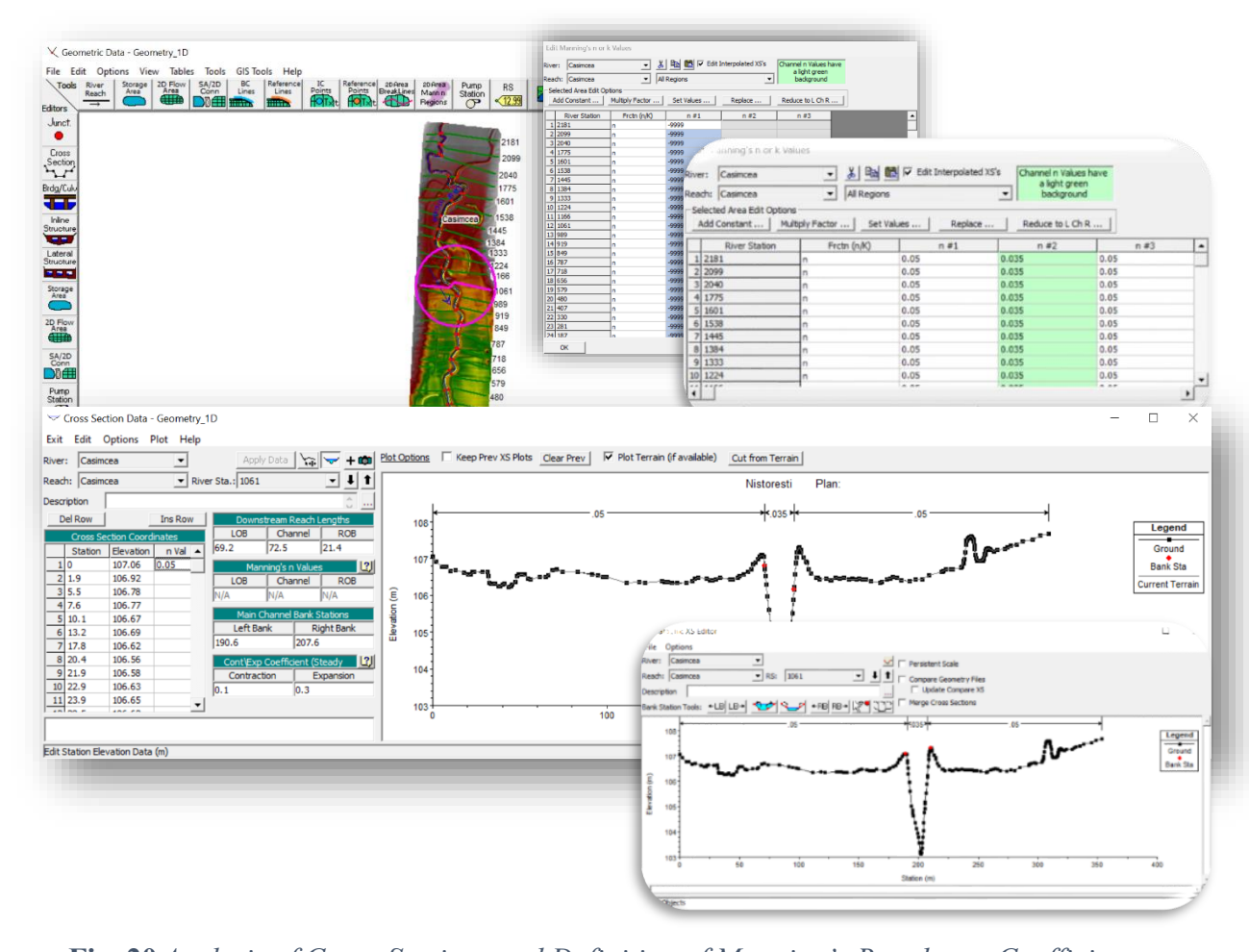
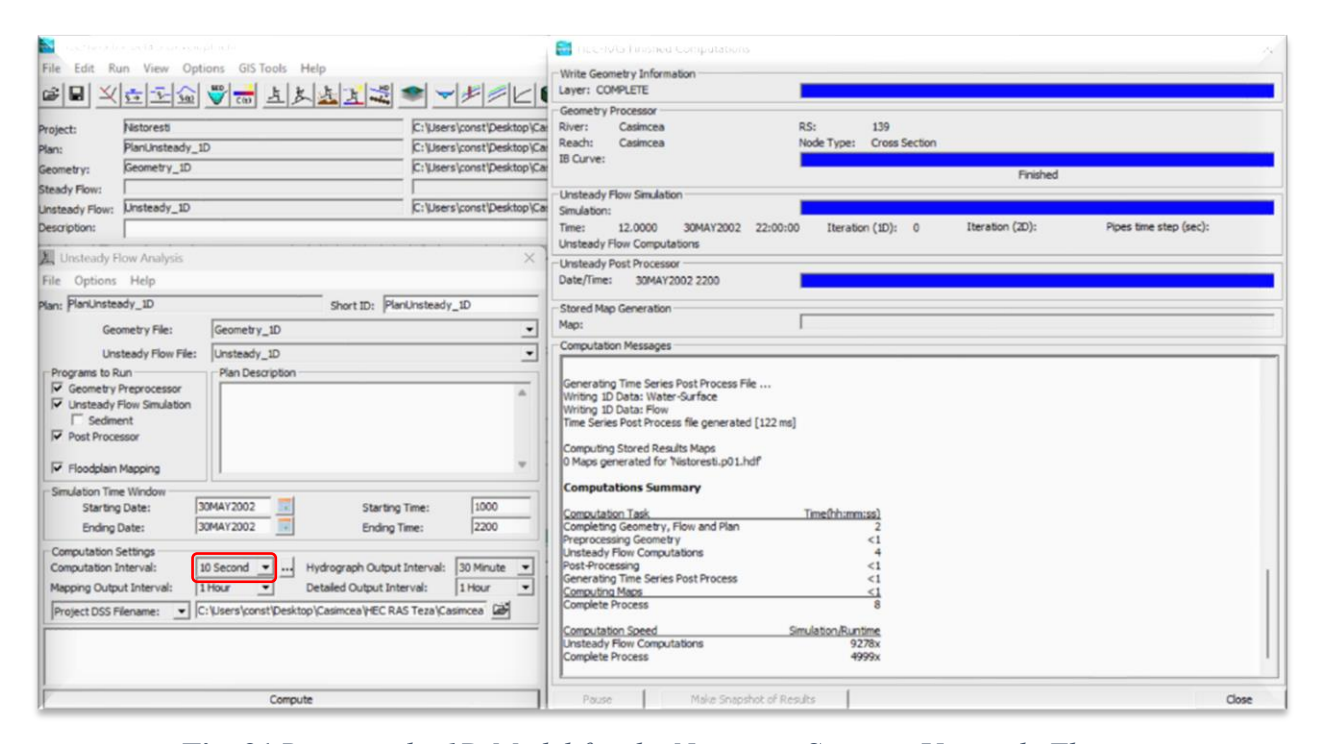


Fig. 20 Analysis of Cross-Sections and Definition of Manning's Roughness Coefficient



**Fig. 21** Running the 1D Model for the Nistorești Sector – Unsteady Flow

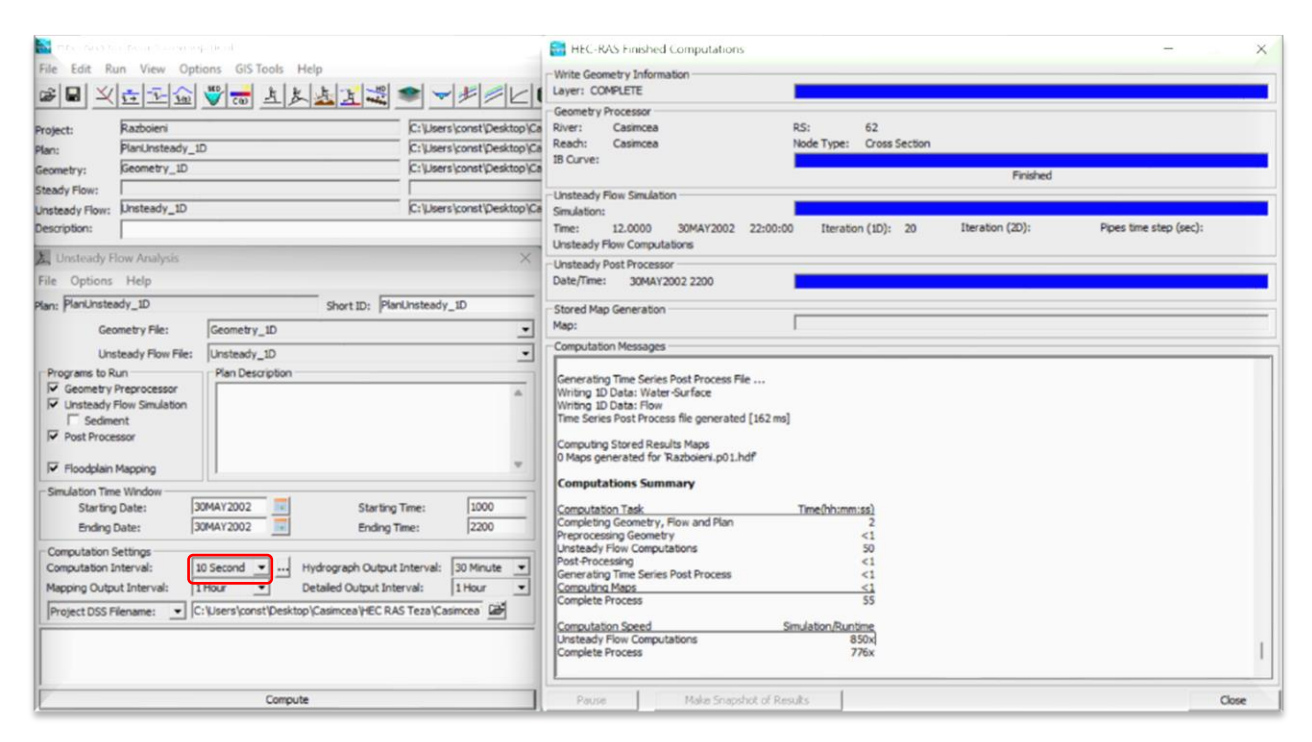


Fig. 22 Running the 1D Model for the Războieni Sector – Unsteady Flow

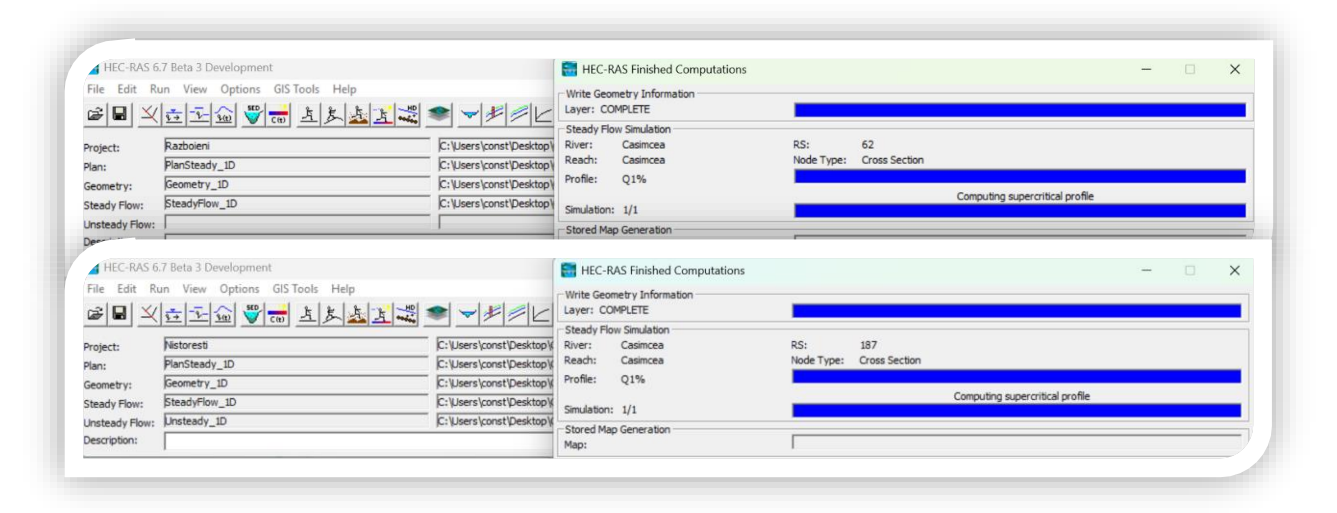


Fig. 23 Results of the 1D Model – Steady Flow

Completing the 1D modeling stage enables flexible management of both data export and import for interpreting results. Flood maps generated by the program, along with outputs in the form of graphs and tables (e.g., velocities, discharges, water levels, flooded areas), can be exported in various formats compatible with GIS and graphic processing software. Similarly, spatial entities (points, lines, polygons), such as administrative boundaries, infrastructure, or reference points, can be imported to verify their alignment with the computed flood extent.

# 6.3. Two-Dimensional (2D) Modeling

2D modeling in HEC-RAS allows the simulation of water flow in two directions (longitudinal and lateral), providing a more detailed and realistic representation of flooding in large

areas or those with complex topography. This approach uses a Digital Elevation Model (DEM) and a computational mesh to analyze the distribution of depth, velocity, and flow direction. It is particularly suitable for urban areas, floodplains, or wide valleys where flow paths are not clearly defined.

For this study, in order to understand flood behavior based on past events and to compare with flood limits extracted from PPPDEI, the 2D modeling was conducted following these steps.

- 1. Creation of 2D Geometry Using the existing terrain in RAS Mapper, a 2D geometry polygon was drawn within the DEM boundaries to encompass at least the flood limits obtained from the 1D model.
- 2. Defining the Computational Mesh The mesh cell size was set relative to the study area and required accuracy. For this study, a 10x10 m cell size was chosen as optimal.
- 3. Model Refinement:
  - The thalweg axis of the channel was defined to align cells with the main flow direction.
  - Smaller cell sizes were applied to the minor channel for greater detail near the thalweg and banks.
  - Structures in the study area were added where necessary. In this case, only the bridge at Nistoreşti was relevant. A preliminary run showed that its abutments and hydraulic opening were sufficient for the 1% discharge, so further adjustments were not required.
  - Mesh errors (e.g., cells with more than eight faces) were corrected by adding new cell centers either manually or automatically using the "Try to Fix All Meshes" function.
- 4. Defining Hydraulic Roughness Coefficients Manning's roughness coefficients were assigned spatially using polygons derived from the Corine Land Cover database. Each land use class was associated with a standard Manning value, adapted to local characteristics for more realistic flow representation.
- 5. Defining Boundary Conditions:
  - Upstream Boundary: The hydrograph used in the 1D model was applied within the minor channel area, distributed across the section to simulate overbank flooding from channel overflow.
  - Downstream Boundary: Three conditions were set according to the terrain slope for each zone: minor channel, left floodplain, and right floodplain. Care was taken to avoid overlapping cells and to place these conditions only outside the analyzed polygon.

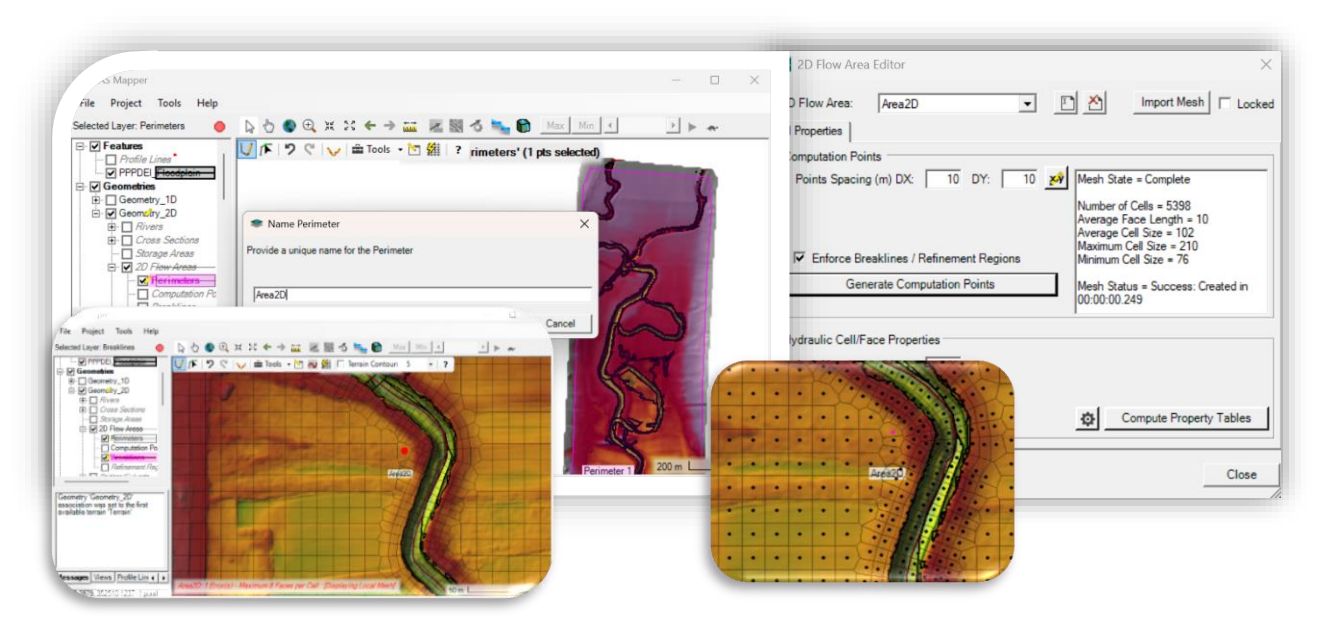


Fig. 24 Creation of 2D Geometry and Refinement of the Computational Mesh – Nistorești Area

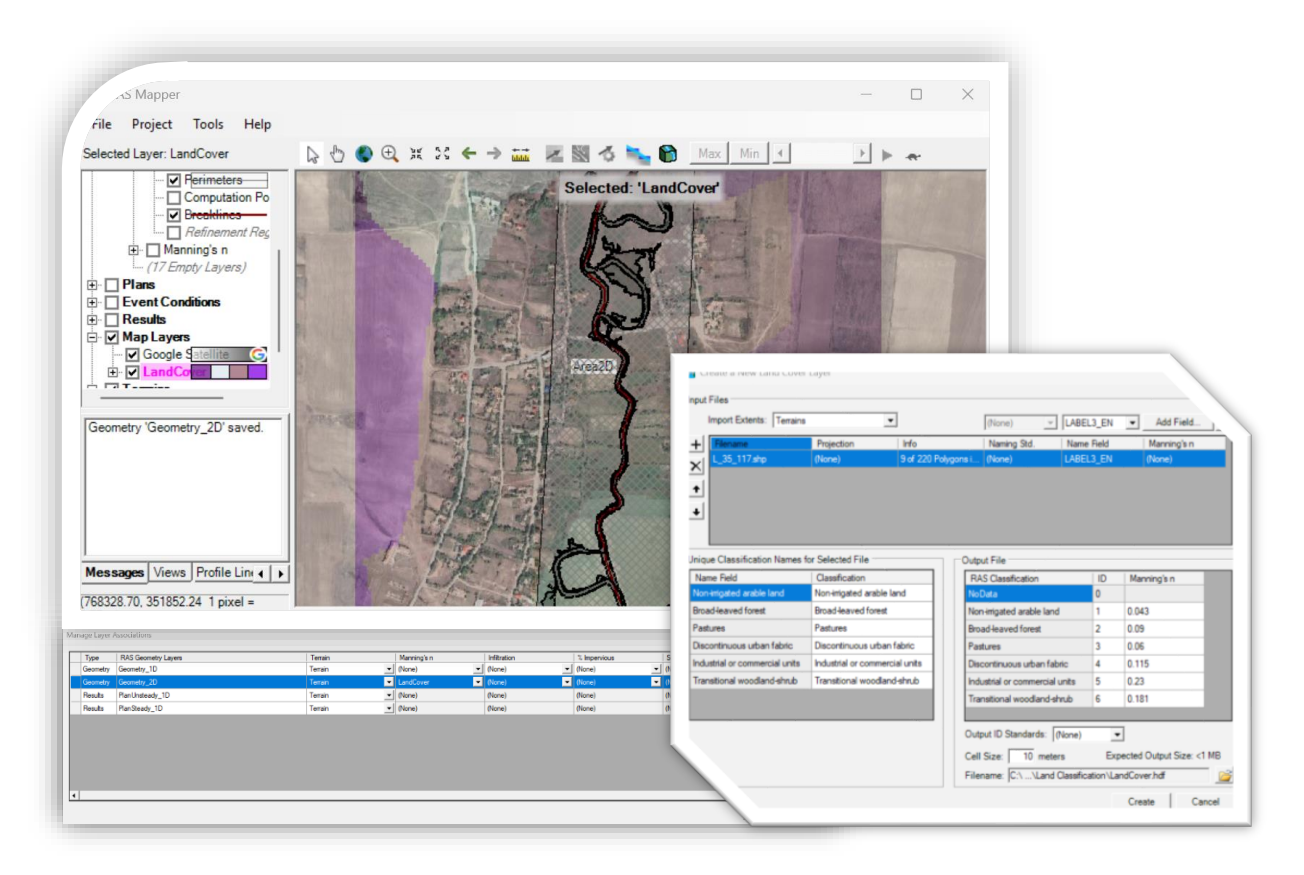


Fig. 25 Assignment of Roughness Coefficients Based on Land Use

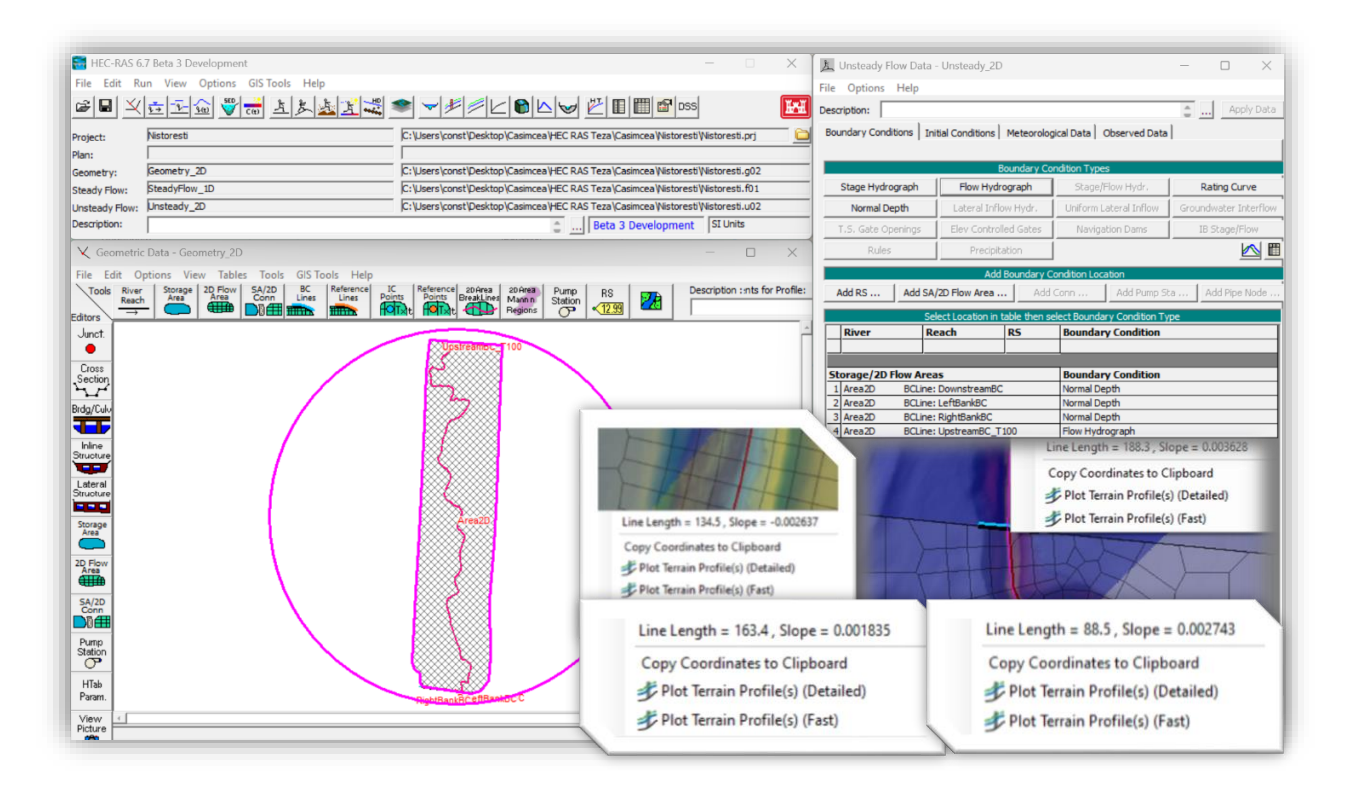


Fig. 26 Definition of Boundary Conditions

Once the boundary conditions are defined, the 2D model simulation is executed, with the time step carefully set, as it is essential for ensuring the stability and accuracy of the model.

# CHAPTER VII RESULTS

# 7.1. Results of Flood Frequency Analysis

The results presented in this chapter have been published in the following scientific works authored by the researcher:

- Flood frequency analysis of Casimcea river. 2021 [27]
- Predictive Modeling of Flood Frequency Utilizing Analysis of Casimcea River in Romania. 2025 [75]

For this analysis, the series of annual peak discharges was used for the period 1965–2021 at three hydrometric stations (Casimcea, Cartal, and Râmnic) and for 1988–2021 at the Cheia station).

## 7.1.2. Analysis of Annual Peak Discharges

The hydrographs of annual peak discharges for the four investigated hydrometric stations are presented in next figure (Fig. 27), and Tab. 4 resents the geographical and hydrological information related to the analyzed hydrometric stations..

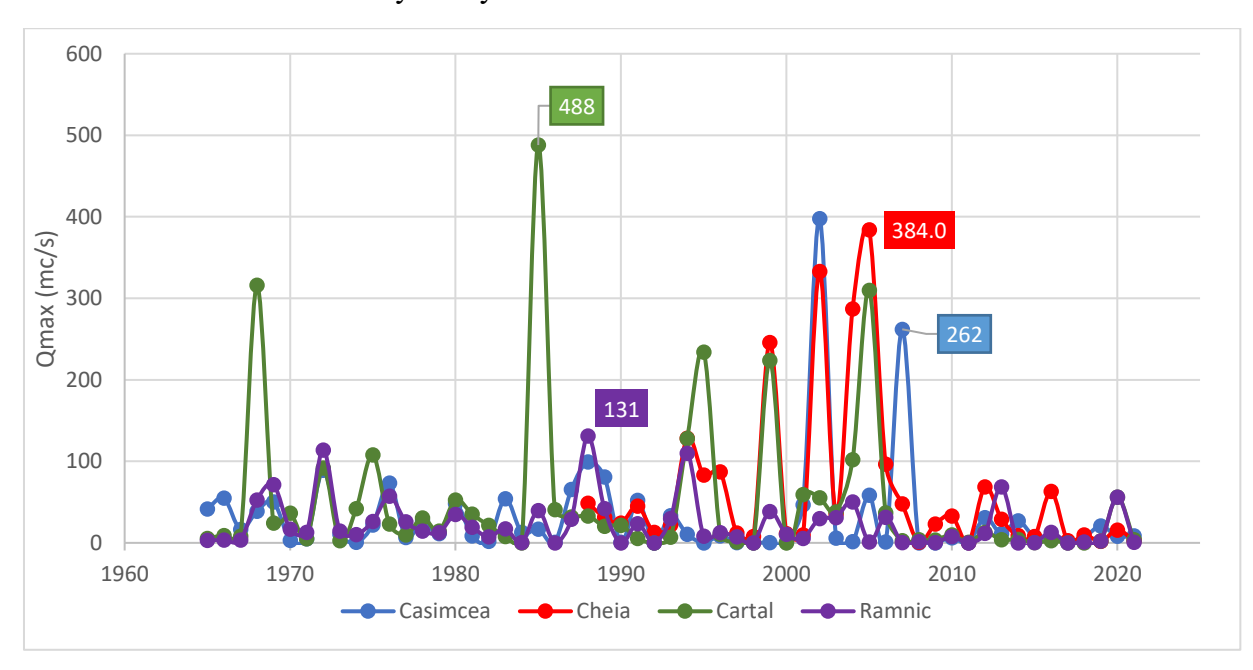


Fig. 27 Hydrograph of Annual Peak Discharges

The discharge measurements began in 1965 (57 years) for the hydrometric stations Casimcea, Cartal, and Râmnic, and in 1988 (34 years) for the Cheia hydrometric station.

The highest recorded discharge was 488 m<sup>3</sup>/s (**Fig. 27**) at the Cartal station in 1985 (**Tab. 4**).

Across all investigated stations, it was observed that the maximum mean discharge values were exceeded between 1994 and 2007. Notably, at the Cartal station, in 1968 and 1985, discharges were recorded that exceeded the mean value by 6 times and 9 times, respectively.

The evolution of the time series shows similar behavior, with some exceptions:

In 1968 and 1985, at Cartal station, two extreme values of 316 m<sup>3</sup>/s and 488 m<sup>3</sup>/s were recorded, while at all other stations, values remained below 100 m<sup>3</sup>/s.

Unfortunately, during 1965–1991, the Cheia station was not operational, preventing comparisons.

Another anomaly was noted in 2002 at Cheia station, where a discharge of 333 m<sup>3</sup>/s was recorded, while at all other stations, values ranged only between 29 and 52 m<sup>3</sup>/s.

In 2005 and 2007, discharges reached 310 m³/s at Cartal and 262 m³/s at Casimcea, while Cheia station registered only 24 m³/s and 48.1 m³/s.

Hydrometric station	Leng of record years	Q mean (m <sup>3</sup> /s)	Q max/data (m <sup>3</sup> /s)	Q min (m <sup>3</sup> /s)	Standard deviation	Skewness	Drainage area (km²)	Average elevation (m)
Casimcea	57	32.43	398/2002	0.048	64.54	4.27	78	263
Cheia	34	65.9	384/2005	0.5	99.70	2.18	500	158
Cartal	56	49.9	488/1985	0.1	92.86	3.06	128	150
Râmnic	56	23.5	131/1988	0.076	29.61	1.98	89	166

**Tab. 4** Recorded discharge limits at the hydrometric stations

The following section presents the results obtained from the analysis of the peak discharge series of the Casimcea River and its tributaries.

## 7.1.2. Results of the Frequency Analysis

As mentioned in the previous sections, determining the exceedance probability of discharges on the Casimcea River is essential for floodplain mapping. A frequency analysis was applied to calculate discharges corresponding to exceedance probabilities of 10%, 1%, and 0.1%.

### Histograms from the Analyses

The following figures (Fig. 28, Fig. 29, Fig. 30 and Fig. 31) present histograms for each hydrometric station.

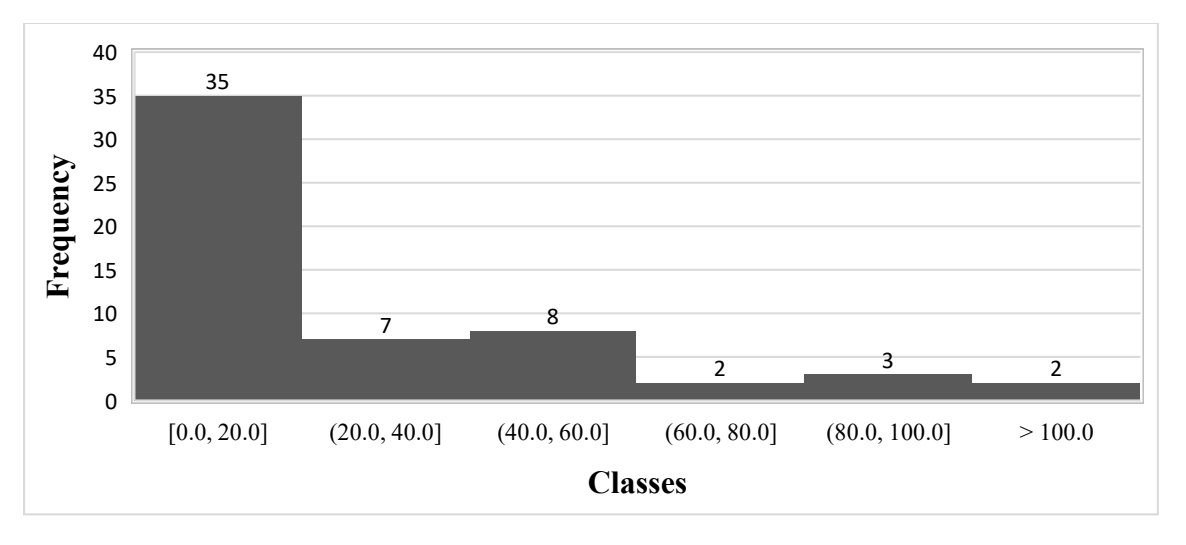


**Fig. 28** *Histogram of Peak Discharges – Casimcea Hydrometric Station (1965-2021)* 

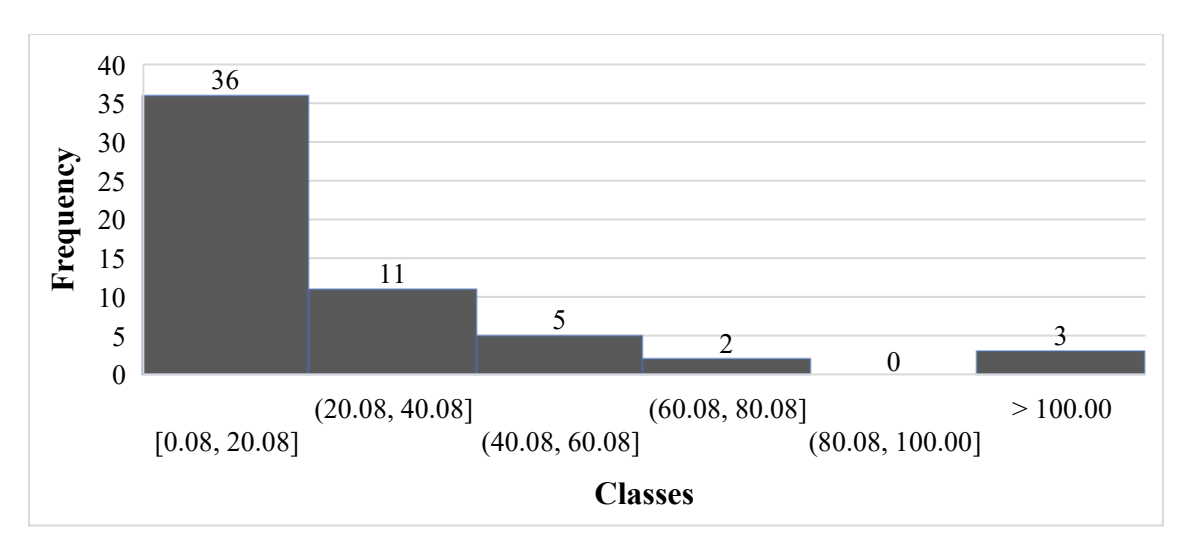


Fig. 29 Histogram of Peak Discharges – Râmnic Hydrometric Station (1965-2021)

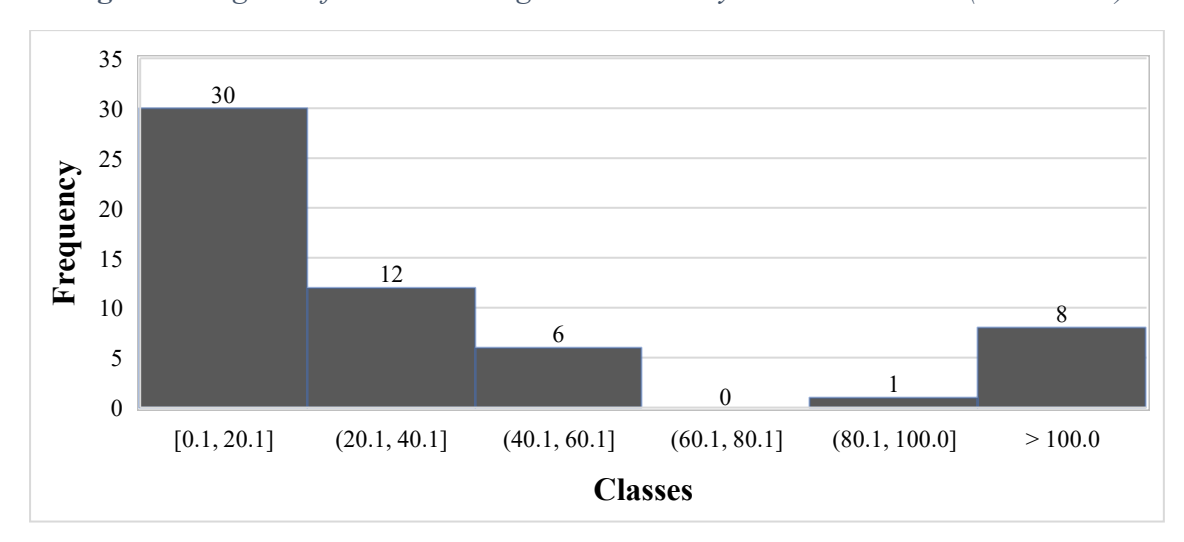


Fig. 30 Histogram of Peak Discharges – Cartal Hydrometric Station (1965-2021)

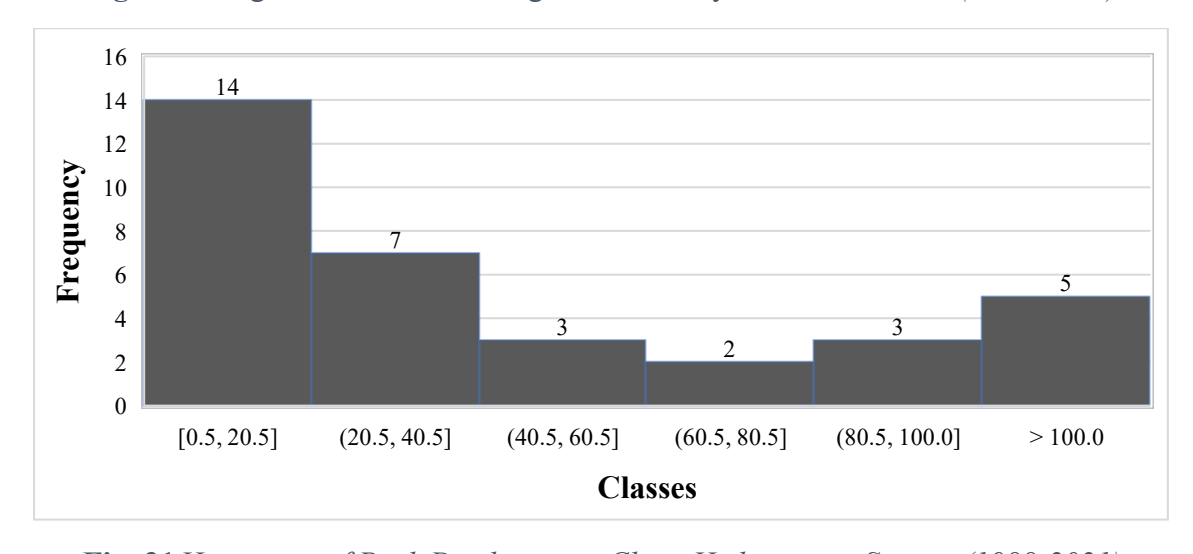


Fig. 31 Histogram of Peak Discharges – Cheia Hydrometric Station (1988-2021)

• All histograms show right-skewness (the tail extends to the right), indicating that most data points are concentrated in the lower discharge range.

- The majority of events occur within the 0–20 m³/s range, accounting for 41% (Cheia station) to 61% (Râmnic station) of observations.
- High-flow events exceeding 100 m<sup>3</sup>/s vary across stations:
  - At Casimcea and Râmnic, there is only one and three such events respectively, each representing less than 5% of all cases.
  - At Cheia and Cartal, these events account for just over 12% of the total.

Based on the descriptions provided in the paragraphs above, the most suitable theoretical probability distribution functions (PDFs) for these events are likely from the Weibull and Log-Normal families.

## Results of Statistical Tests

## **Trend Estimation**

As mentioned in Chapter III, we investigated trends and breakpoints in the peak discharge series. For trend detection, the MAKESENS program was used, while the Khronostat software was applied to identify breakpoints within the time series.

Four significance levels (α) were tested using MAKESENS: 0.001, 0.01, 0.05, and 0.1.

All time series analyzed exhibited similar behavior, indicating consistent patterns across the studied stations. **Fig. 32** provides a graphical example of the trend analysis results for the Casimcea station.

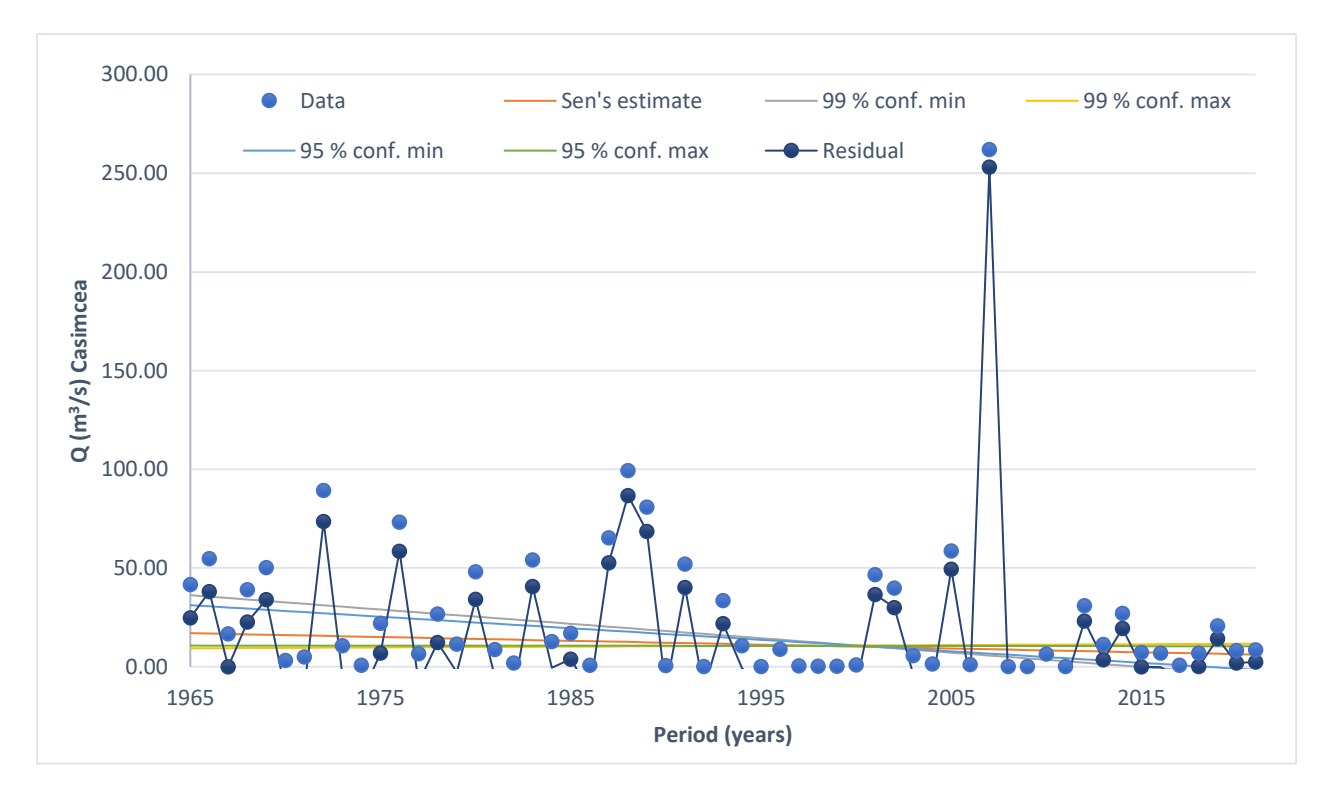


Fig. 32 Result of the Mann-Kendall Test for Casimcea Station

## **Breakpoints Estimation in Time Series**

The Khronostat program, developed by IRD Montpellier (Research Institute for Development), was initially designed as part of a study on climate variability in West and Central Africa, with a focus on the analysis of hydrometeorological time series [20].

This software includes the following statistical tests:

- Stationarity tests: autocorrelation test, rank correlation test
- Homogeneity tests: Pettitt test, Buishand test, Hubert test, and the Bayesian method of Lee & Heghinian

These tests were described in Chapter III.

Table **Tab.** 5 presents the results of the statistical tests conducted in Khronostat. Notably, the Pettitt, Lee & Heghinian, and Hubert tests also indicate the year in which a breakpoint occurred within the time series for each analyzed station.

Station	Period	Mean (m <sup>3</sup> /s)	Rank correlation	Buishard	Pettitt		Lee Heghii		Hubert
	(years)	(111-78)	correlation		Result	year	Result	year	Result
Casimcea	57	26.03	rejected at 95% confid.	rejected at 95% confid.	rejected at 95% confid.	1989	rejected Ho	1989	accepted
Cheia	34	55.0	rejected at 95% confid.	rejected at 95% confid.	rejected at 95% confid.	2007	rejected Ho	2007	accepted
Cartal	57	50.8	rejected at 95% confid.	rejected at 95% confid.	rejected at 95% confid.	2006	rejected Ho	2006	accepted
Ramnic	57	23.9	rejected at 90% confid.	rejected at 90% confid.	rejected at 90% confid.	2006	rejected Ho	2006	accepted

**Tab. 5** *Independence test results of the time series for all investigated stations.* 

The results indicate that the investigated time series data are not random at a 95% confidence level (significance levels of 0.1 and 0.05) and may exhibit a trend or periodicity.

Analysis of the data from **Tab.** 5 shows:

- Buishand, Pettitt, and Lee & Heghinian tests reject the null hypothesis at a significance level of 0.05 for Casimcea, Cheia, and Cartal, and at 0.1 for the Râmnic hydrometric station.
- Hubert tests accepted the null hypothesis.
- Two of the three tests providing a breakpoint year detected breaks: 2006 for Casimcea and Râmnic, 2007 for Cheia, and 1989 for Casimcea.

The discharge data series analyzed are therefore not evidently homogeneous. According to Lee & Heghinian tests, the break is most severe at Cheia station (breakpoint probability: 0.4131), followed by Casimcea (0.0738), Cartal (0.1616), and Râmnic (0.1175).

## Selection of the Empirical Frequency Model (EDF - Empirical Distribution Function)

To select the frequency model, the Flow Duration Curve (FDC) was used, determined with two empirical cumulative frequency functions (EDF): Hazen and Weibull.

• Both Weibull and Hazen EDFs were applied to all four time series.

• The discharge values derived from theoretical distribution functions (PDFs) were then compared to those obtained for return periods of 100, 50, 20, 10, 5, and 2 years using the Hazen and Weibull equations (**Tab.** 6).

**Tab. 6** Maximum discharge values for all stations

Maximum discharge (m <sup>3</sup> /s)										
Return period (year)	100	50	20	10	5	2				
EDF	Hazen									
Casimcea	262	157.87	89.3	65.4	50.3	10.7				
Cheia	no	377.92	310	128	56.2	12.9				
Cartal	333	324.72	287	246	83.1	24.3				
Ramnic	131	119.85	110	57.2	39.8	12.6				
EDF	Weibull									
Casimcea	262	224.35	99.3	73.3	50.3	10.7				
Cheia	no	333	297.87	246	83.1	24.3				
Cartal	488	460.48	316	224	56.2	12.9				
Ramnic	131	128.12	114.00	68.8	39.8	12.6				

## Selection of the Theoretical Frequency Model (PDF - Probability Density Function)

In a recent study, Cerneagă C. et al. (2021) [27], several frequency models were analyzed using Hydrognomon, a software designed for hydrological data processing. This open-source application runs on standard Microsoft Windows platforms and is part of the openmeteo.org framework.

The distribution functions most frequently recommended in the literature—Log-Normal, Pearson Type III, Log-Pearson Type III, and Gumbel—were tested for the annual maximum discharge time series available up to 2016, at the time of the analysis.

Two statistical goodness-of-fit (GOF) tests were applied:

- Kolmogorov-Smirnov (K-S) using Hydrognomon, and
- Anderson-Darling (A-D) using EasyFit.

The Log-Pearson Type III distribution was accepted statistically; however, the discharge values obtained for different return periods were significantly higher compared to those calculated using empirical formulas.

## Conclusion and Alternative Approach

Due to this overestimation, the usual theoretical distributions for maximum discharges were deemed unsuitable. Consequently, additional distribution functions were tested.

The proposed method involved using Hydrognomon's K-S test as a statistical GOF test to verify whether a sample fits a specified population distribution.

- For the Casimcea station, **Tab.** 7 presents the detailed results.
- **Tab. 8** lists the PDF functions with the best fit for all hydrometric stations analyzed.

**Tab.** 7 Results of the K-S Test for the Casimcea Hydrometric Station

Kolmogorov-Smirnov/PDF	a=1%	rank	$\mathbf{D}_{max}$
Gamma	ACCEPT	1	0.0796
Pearson III	ACCEPT	2	0.0831
GEV-Min	ACCEPT	3	0.0847
EV3-Min (Weibull, L-Moments)	ACCEPT	4	0.098
EV3-Min (Weibull)	ACCEPT	5	0.1052
Pareto (L-Moments)	ACCEPT	6	0.1200
GEV-Min (L-Moments)	ACCEPT	7	0.1215

**Tab. 8** Accepted PDF Functions in Order of Rank

PDF Station	Gamma	Pearson III	GEV-Min	EV3-Min (Weibull, L- Moments)	EV3-Min (Weibull)	Pareto (L- Moments)	GEV-Min (L- Moments)	GEV-Max (L- Moments)	Log Pearson III
Casimcea	1	2	3	4	5	6	7	X	X
Cheia	7	X	X	6	3	1	4	2	5
Cartal	7	X	6	2	1	5	5	4	3
Ramnic	2	X	X	5	6	3	4	1	X

Next, we compared the maximum discharge values obtained by fitting the valid PDF functions for all hydrometric stations with those derived from the EDF functions. An example is provided for the Casimcea station, where the maximum discharge values estimated using the selected PDFs and the EDF values corresponding to the return periods are presented in **Tab. 9**.

**Tab. 9** Comparison between PDF and EDF values at the Casimcea hydrometric station

Return period (T) PDF's	1000	100	50	50 20		5	2
	(	Casimcea -	- Qmax (m	<sup>3</sup> s)			
Gamma	323.52	193.42	155.81	107.94	73.83	42.63	9.94
EV3-Min (Weibull, L-Moments)	376.84	201.90	157.07	104.16	69.47	40.032	10.95
EV3-Min (Weibull)	361.02	196.20	153.52	102.77	69.18	40.37	11.37
Pareto (L-Moments)	469.36	200.59	149.70	96.69	65.17	39.53	12.82
GEV-Min (L-Moments)	331.60	187.72	149.21	102.36	70.45	42.15	11.95
EDF		262	157.8	89.3	65.4	50.3	10.7

The most important conclusion is that models cannot be selected solely based on the ranking value.

This is why we used a series of coefficients to determine the error between the modeled and observed values. The Pearson correlation coefficient (r), RMSE (Root Mean Square Error), NSE (Nash-Sutcliffe Efficiency coefficient), and  $R^2$  (Coefficient of Determination) are used to assess the performance of the PDF models..

**Tab. 10** Calibration results – observed values for exceedance probability are extracted using the Hazen and Weibull equation

			Hazen			Weibull			
	rank	r	RMSE	NSE	R <sup>2</sup>	r	RMSE	NSE	$\mathbb{R}^2$
			Casimcea	l	1				
Gamma	1	0.96	29.40	0.87	0.92	0.98	39.87	0.81	0.92
EV3-Min (Weibull, L-Moments)	2	0.97	25.68	0.90	0.95	0.98	37.15	0.84	0.95
EV3-Min (Weibull)	3	0.97	27.82	0.89	0.94	0.98	39.74	0.81	0.94
Pareto (L-Moments)	4	0.98	25.86	0.90	0.97	0.99	39.87	0.81	0.97
GEV-Min (L-Moments)	5	0.97	31.24	0.86	0.94	0.98	43.30	0.78	0.94
			Cheia						
Pareto (L-Moments)	1	0.87	73.34	0.62	0.76	0.93	56.67	0.74	0.87
EV3-Min (Weibull)	2	0.90	80.06	0.55	0.80	0.94	56.91	0.74	0.88
GEV-Min (L-Moments)	3	0.92	52.44	0.81	0.85	0.93	53.70	0.77	0.86
EV3-Min (Weibull, L-Moments)	4	0.90	60.02	0.75	0.81	0.82	172.03	-1.40	0.67
Gamma	5	0.90	60.02	0.75	0.81	0.94	53.91	0.76	0.88
			Cartal						
EV3-Min (Weibull)	1	0.98	49.00	0.92	0.80	0.97	79.97	0.81	0.93
EV3-Min (Weibull, L-Moments)	2	0.98	38.52	0.75	0.81	0.98	67.81	0.86	0.92
Pareto (L-Moments)	3	0.96	58.72	0.62	0.76	0.96	92.35	0.74	0.86
GEV-Min (L-Moments)	4	0.97	45.35	0.81	0.85	0.97	72.52	0.84	0.91
Gamma	5	0.99	40.54	0.75	0.81	0.99	68.58	0.86	0.96
	Râmnic								
Gamma	1	0.86	37.36	0.29	0.74	0.83	38.43	0.28	0.70
Pareto (L-Moments)	2	0.79	68.69	-1.41	0.62	0.75	69.22	-1.33	0.57
GEV-Min (L-Moments)	3	0.87	34.92	0.38	0.76	0.82	46.06	-0.03	0.67
EV3-Min (Weibull, L-Moments)	4	0.82	61.21	-0.91	0.68	0.79	44.37	-0.84	0.63
EV3-Min (Weibull)	5	0.84	43.35	0.04	0.71	0.81	61.55	0.04	0.66

The results presented in the table above (**Tab.** 10) show that:

- (i) the correlation coefficients (r) yield good results, close to the value of 1, indicating an excellent correlation between the observed and modeled values; there are some exceptions: at the Râmnic station, the r value ranges between 0.79 and 0.87, allowing us to conclude that there is a strong positive linear relationship between the observed and modeled peak discharge values;
- (ii)  $R^2$  also provides good results for the Casimcea station, while for the other stations,  $R^2$  values exceed 0.85; an  $R^2 > 0.5$  is generally considered satisfactory;
- (iii) NSE yields some values close to 1 or even negative; an NSE close to 1 indicates that the model estimates are as accurate as the mean of the observed data, whereas negative NSE values reflect unacceptable performance;
- (iv) RMSE values should be interpreted with caution. The RMSE error ranges between 25.68 m³/s and 172.03 m³/s. PDF models with the lowest RMSE values achieved the best results. RMSE uses the same units as the dependent variable (m³/s) and is sensitive to outliers.

The results obtained by applying the error functions, presented in **Tab.** 10, are consistent with those derived from the probability plots.

The confidence interval (CI) was also determined. In the following figure (**Fig. 33**) it can be observed that the EV3-Min-Weibull (L-moment) function provides results within the CI limits. As expected, the left tail of the PDF lies outside the prediction interval (PI) but remains within the CI ranges.

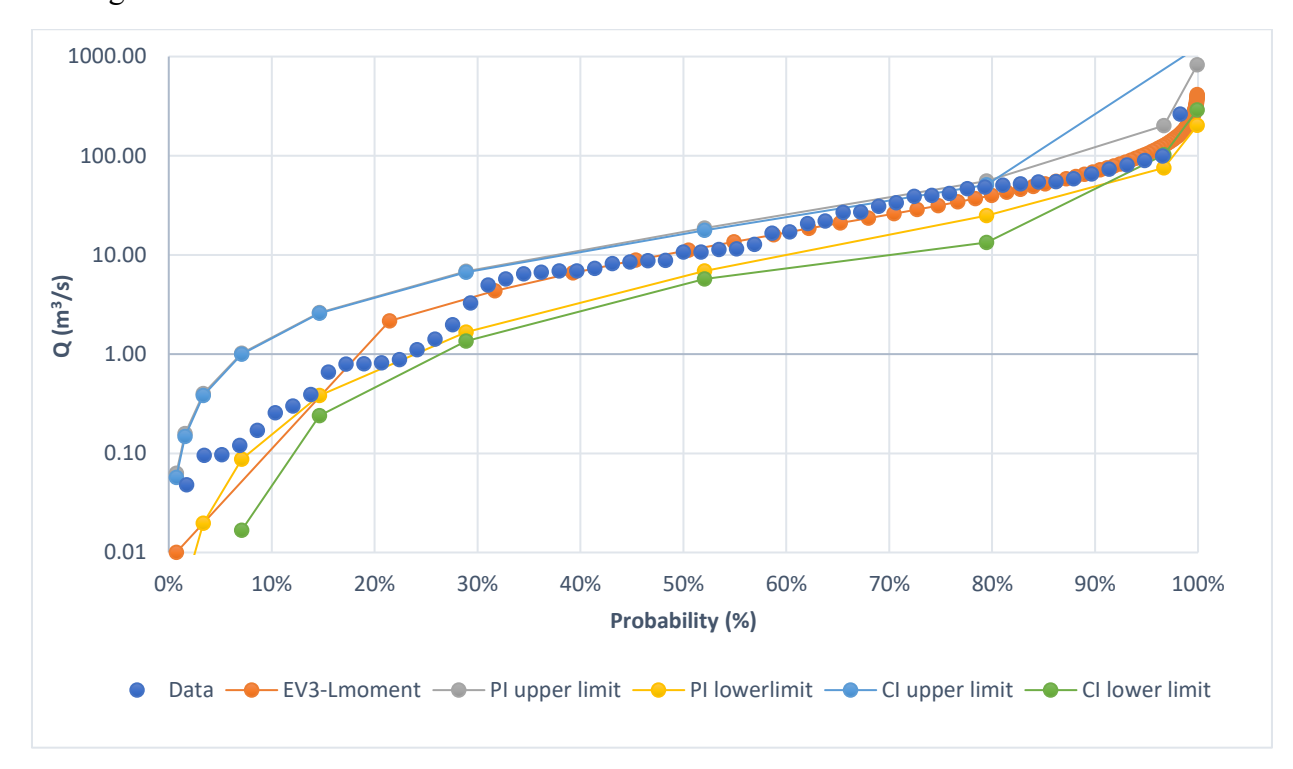


Fig. 33 Performance of the EV3 PDF at the Casimcea Station

In conclusion, no single probability distribution model can be universally applied to the Casimcea River and its tributaries while simultaneously delivering the best statistical performance. A key limitation of this analysis is its reliance on the Kolmogorov–Smirnov test; however, the application of the Anderson–Darling test did not reveal significant differences in the goodness of fit.

The 1D and 2D modeling was performed using discharge values from the PPPDEI, as these values provide a higher safety margin and are considered more representative for design scenarios. In comparison, the discharges estimated through frequency analysis yielded noticeably lower values, which would have led to an underestimation of hydraulic and hydrological risks. The use of PPPDEI discharges ensures a more conservative approach and aligns with the safety requirements mandated by current technical regulations.

Moreover, employing these discharges results in more realistic hazard and risk maps, directly applicable in spatial planning and risk management processes. For this reason, PPPDEI values were preferred over statistically derived ones, offering a more suitable estimate of peak discharges for the analyzed areas.

## 7.2. Results of 1D Modeling

**Nistorești** For the unsteady hydraulic simulation in the Nistorești area, a 1% design hydrograph was applied, testing multiple time-step values (1 minute, 30 seconds, and 10 seconds). Reducing the time step significantly improved the volume balance accuracy, with the percentage error decreasing from approximately 1.45% (at 1 minute) to 0.15% (at 10 seconds) - **Error! Reference source not found.**.

Below are the results regarding the distribution of flow velocities and discharges (Fig. 34) or the Nistorești sector.

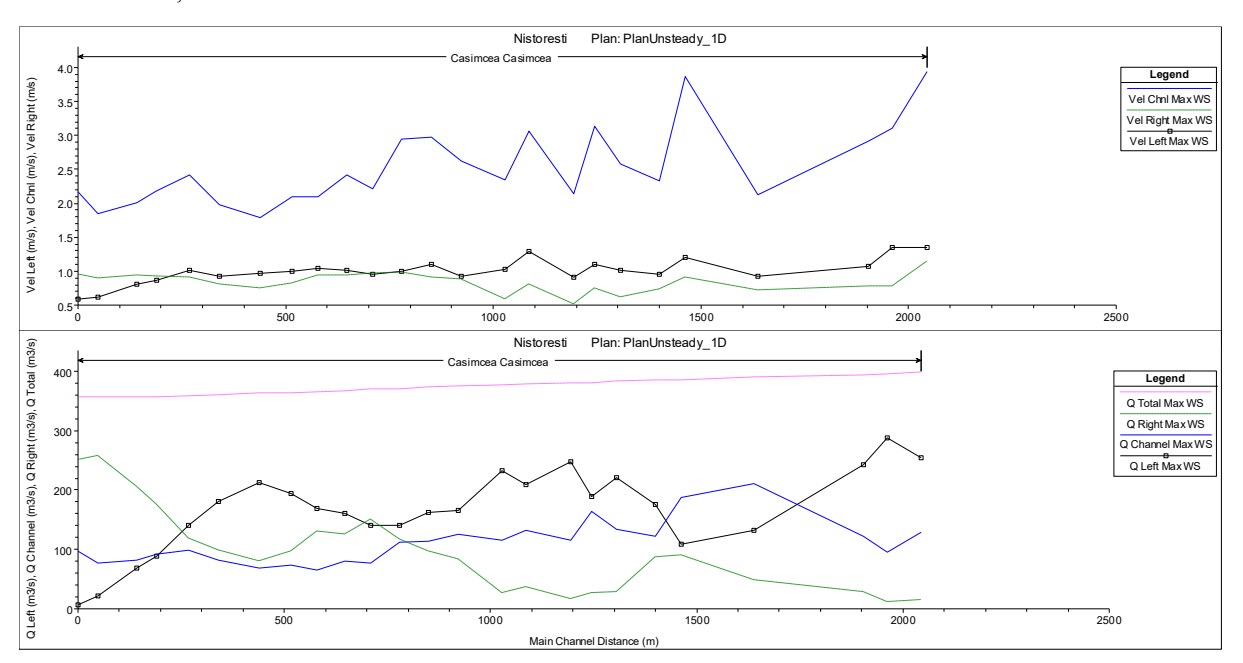
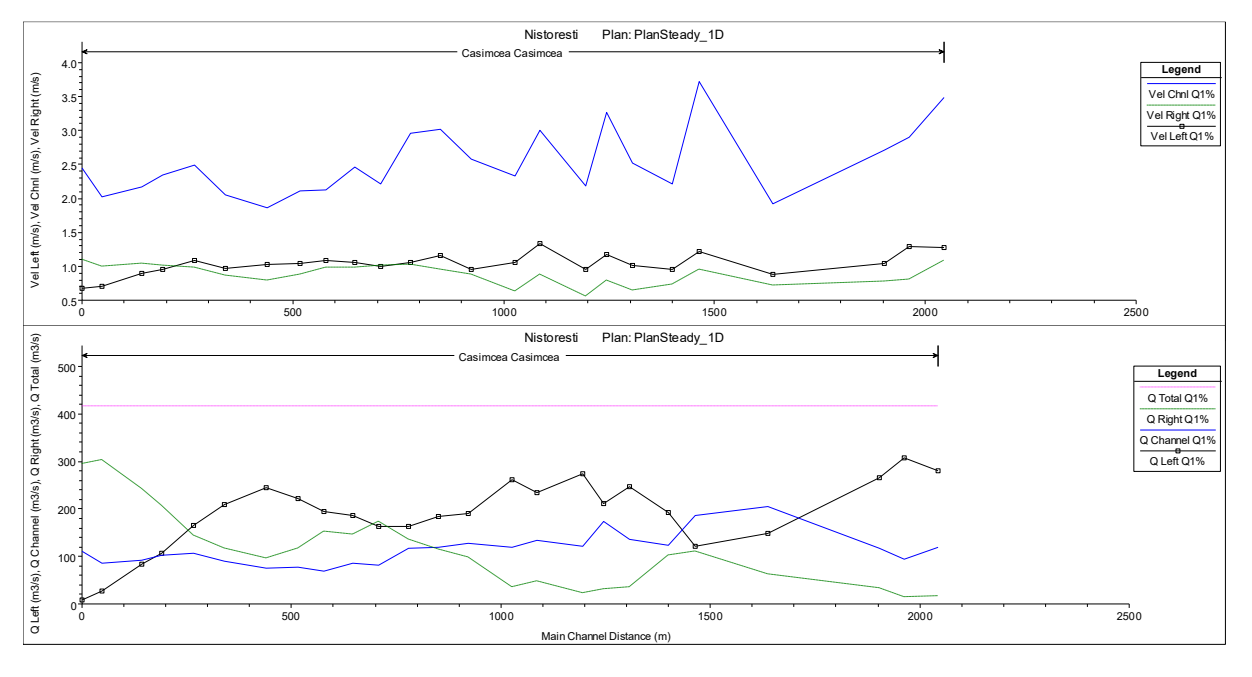


Fig. 34 Distribution of velocities and discharges under unsteady flow – Nistorești



**Fig. 35** *Distribution of velocities and discharges under steady flow – Nistorești* 

It can be observed that, under unsteady flow conditions, the water velocity in the minor riverbed exceeds 3.8 m/s in certain cross-sections, indicating localized accelerations caused by discharge variations and the propagation of flood waves. In the inundated areas, the velocity on the left bank generally remains between 0.6 and 1.4 m/s, while on the right bank it can reach values of up to 1.5 m/s, highlighting the active involvement of lateral floodplain areas in the flow process under transient conditions.

Compared to the unsteady flow regime, under steady flow conditions, the water velocity in the minor riverbed remains between 2.0 and 3.8 m/s, without significant variations along the analyzed section. This uniformity reflects a stable and hydraulically balanced flow, with no local accelerations or abrupt redistributions of the flux. In the temporarily inundated lateral areas, velocity values range between 0.5 and 1.1 m/s on the left bank and between 0.6 and 1.3 m/s on the right bank—typical characteristics of marginal sectors with shallow depths, where the flow energy is progressively dissipated.

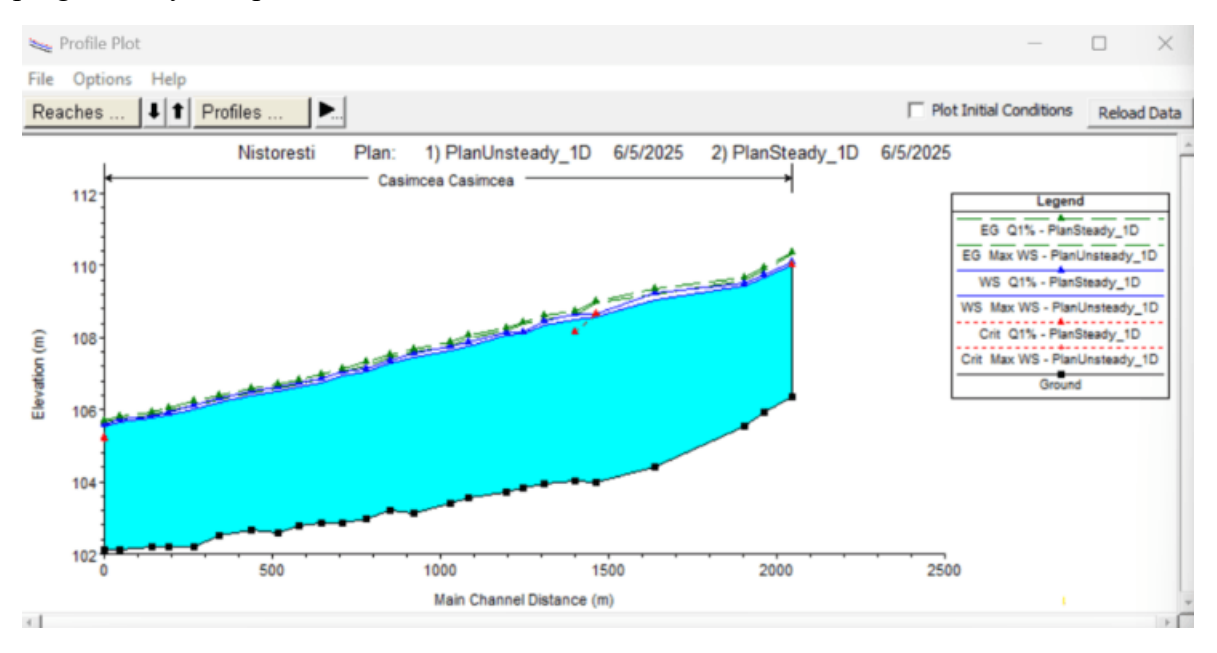


**Fig. 36** Water level in unsteady/steady flow – Nistorești

Thus, the comparative analysis highlights the fundamental differences between the two regimes: from a uniform, geometrically controlled flow in the steady regime to a complex transient behavior in the unsteady regime, influenced by the temporary nature of the flood wave and the local variability of flow conditions. However, as shown in **Fig. 36**, the maximum water levels under the unsteady regime are close to those in the steady regime, with moderate and consistent differences across the entire analyzed sector. This indicates that, although the transient regime generates a slight increase in levels in the lateral floodplain areas, no significant hydraulic instabilities occur, and the flood wave propagates predictably. Consequently, the dynamics of unsteady flow reflect a temporary extension into the adjacent floodplain areas without abrupt regime changes or uncontrolled local behaviors.

**Războieni** In the unsteady hydraulic modeling conducted for the Războieni area, similar to the approach applied at Nistorești, three time step options were tested: 1 minute, 30 seconds, and 10 seconds. Although reducing the time step results in a slight improvement in

accuracy (a difference of only a few cubic meters), this refinement is marginal compared to the additional processing resources required.

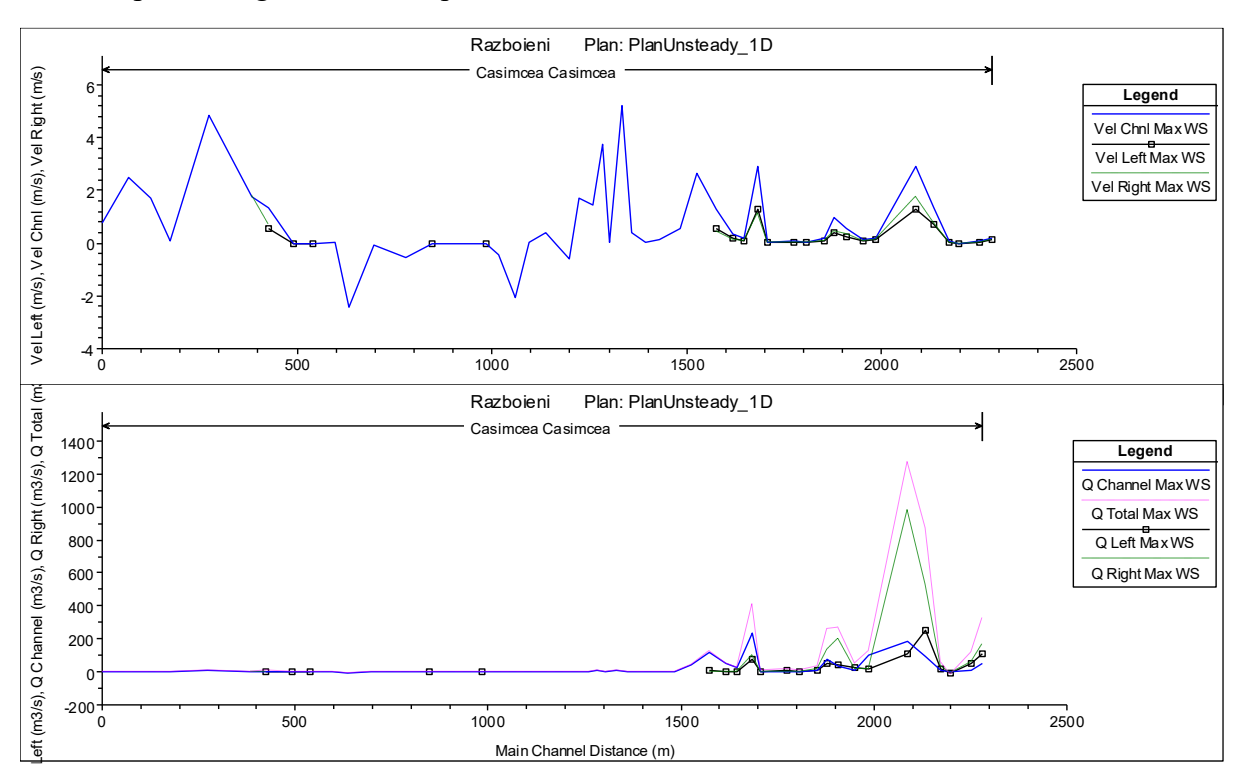


Fig. 37 Distribution of velocities and discharges under unsteady flow – Războieni

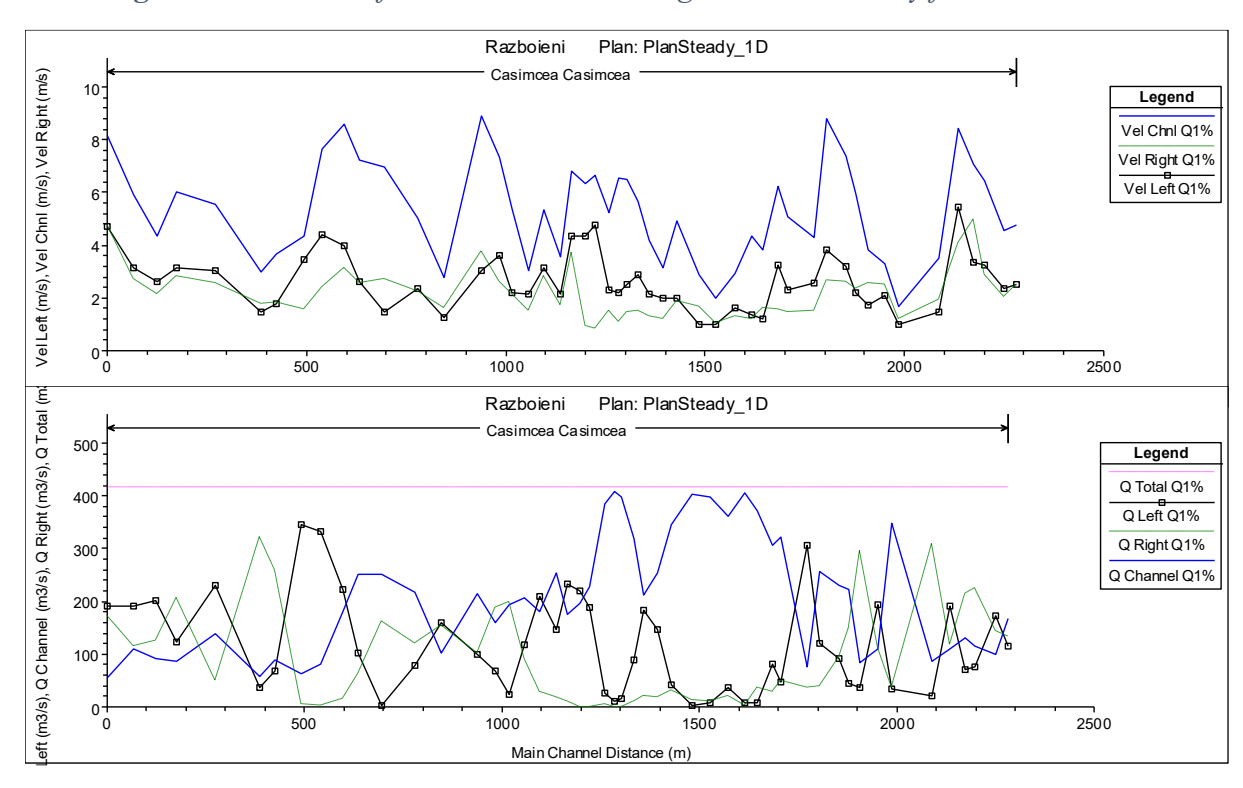


Fig. 38 Distribution of velocities and discharges under steady flow – Războieni

Additionally, the unsteady hydraulic simulation for the Războieni sector highlights significant variability in velocities and discharges along the reach, characteristic of flood wave

propagation. Within the main channel, the maximum velocity reaches 6 m/s, while certain sections even record negative values, indicating local backflows or flow oscillations caused by the unstable dynamics of the wave. In the adjacent floodplain areas along both the left and right banks, velocities remain low, fluctuating between 0 and 2 m/s.

The upstream boundary condition imposed a peak discharge of 398 m³/s; however, downstream (after station 1900), the model revealed peaks reaching up to 1400 m³/s, indicating a substantial amplification of the flood wave during its propagation.

Compared to the simulation performed in unsteady flow, the steady flow simulation corresponding to a 1% exceedance probability discharge reveals a distinctly differentiated distribution of velocities across the cross-section.

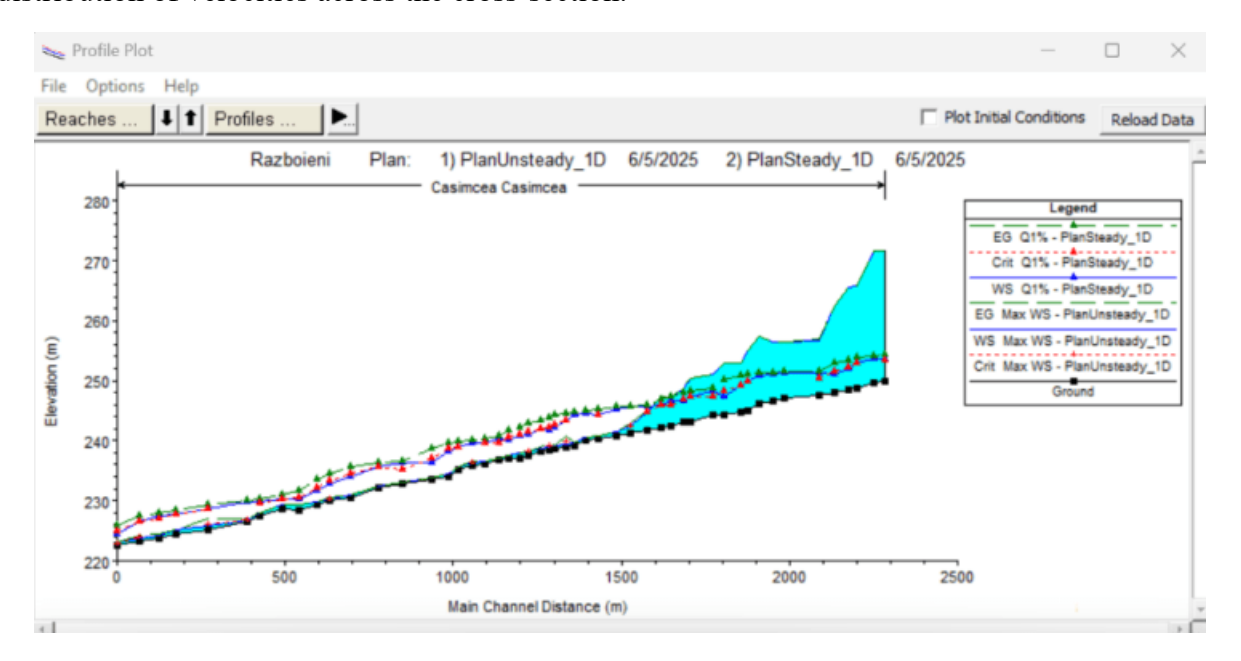


Fig. 39 Water level in unsteady/steady flow – Războieni

Thus, the steady-state regime exhibits a more stable distribution, with high velocities and constant discharges, characteristic of a uniform and well-defined flow under extreme conditions.

In contrast, the unsteady-state regime highlights much greater variability (**Fig. 39**), with areas of backflow, accumulation, and rapid discharge, reflecting a complex river response to a flood wave. However, further analyses are necessary regarding the consistency of the geometric data to confirm whether the observed variations result from inaccuracies in the configuration and calibration of the simulation. It can also be noted that this lack of precision may be caused by the discontinuous nature of the flow, as well as the model's high sensitivity to the geometric configuration of the cross-sections included in the simulation.

# 7.3. Results of 2D Modeling

In the Nistorești area, the simulated scenarios indicate a similar flow distribution, with coherent macro-level results, despite the instability observed in the 1D unsteady model. In the Războieni area, the 2D unsteady modeling and 1D steady-state modeling provide comparable

results regarding flood extent, while the 1D unsteady model highlights instabilities and irregular boundaries, requiring recalibration.

Another important aspect is the correlation between the results obtained from these simulations and those presented in the Flood Prevention, Protection, and Mitigation Plan (PPPDEI).

Moreover, in the context of the second planning cycle of the Flood Risk Management Plan (FRMP) for the Dobrogea-Litoral river basin, as outlined in Chapter II, it was observed that flood hazard boundaries derived from fluvial sources were not updated for inland watercourses. This omission necessitates a re-evaluation in the third planning cycle, particularly for APSFR sectors located within urban areas, using updated data on infrastructure works, hydraulic structures, and recent digital terrain models (DTMs).

Continuing the analysis for the Nistorești area, the methodological steps detailed in Chapter VI were repeated, extending the computational domain for 2D modeling. A new simulation area was defined with a cell size of 100x100 m, compared to the 10x10 m grid used in the previous model.

By maintaining the same spatial resolution of the digital terrain model, the extended model aimed to verify the hydraulic behavior's consistency at a larger scale. The results showed flood boundaries similar to those generated by the initial model, confirming the continuity of flow behavior and the uniformity of topographic and hydraulic characteristics across the analyzed sector.

This finding highlights the hydraulic representativeness of the initial sector, indicating that extending the modeling area did not lead to significant variations in flood extent. Maintaining the DTM resolution across the entire modeled area ensured coherence and comparability of results, demonstrating that a uniform spatial discretization allows for reliable simulations at both local and regional scales (**Fig. 40**).

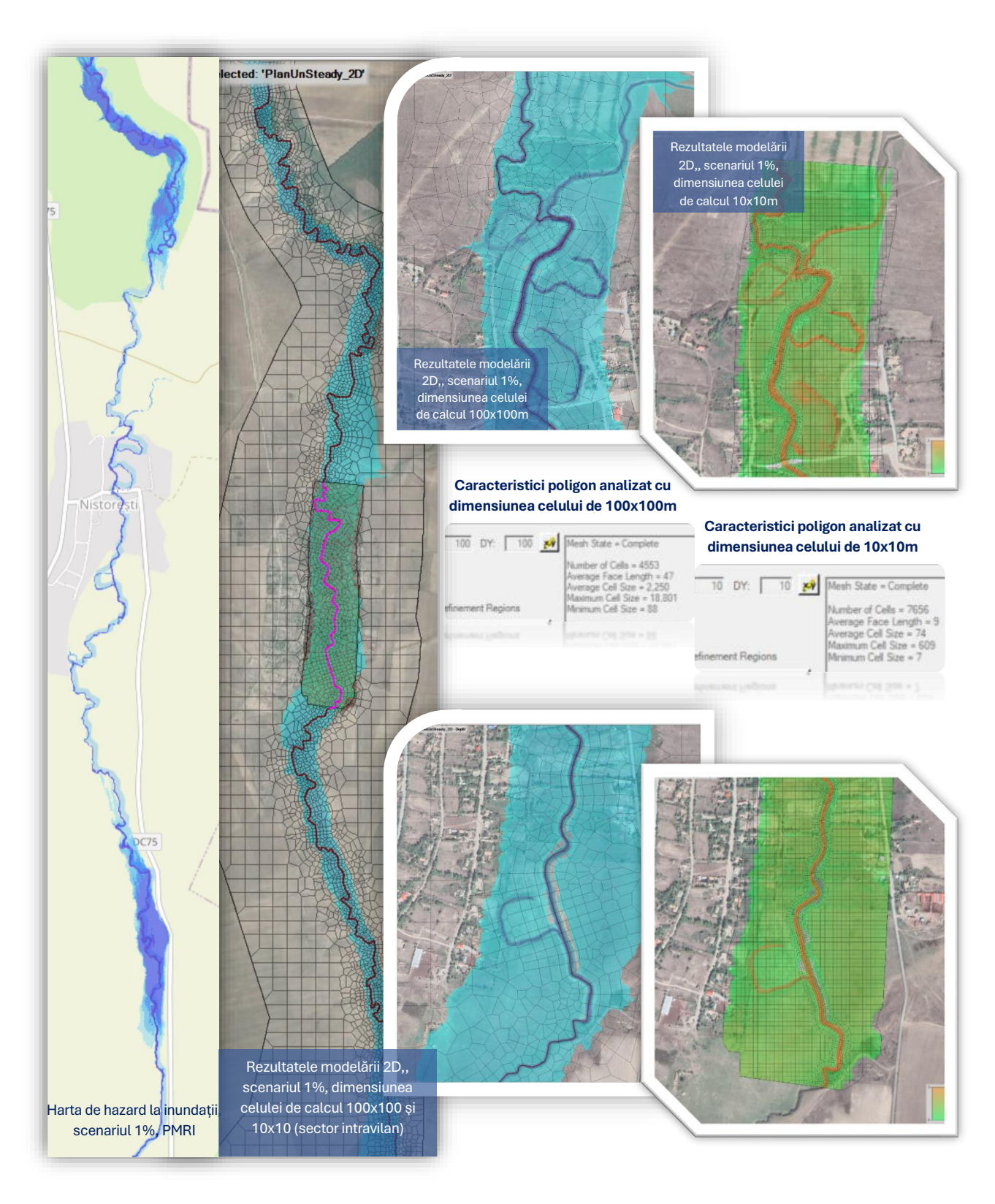


Fig. 40 Results of 2D Modeling Compared to the Flood Hazard and Risk Map Boundaries

## Conclusions, Personal Contributions, and Future Perspectives

Romania completed Cycle II of the Floods Directive implementation at the end of 2023, a process that involved revising the Flood Hazard and Risk Maps (FHRM) and developing the Flood Risk Management Plans (FRMP). This cyclical process (every 6 years) builds on Cycle I of the Directive, where, for the Dobrogea-Litoral river basin, a hydrological model was created using MIKE SHE over an area of 1,076 km², complemented by a hydraulic model developed in MIKE 11 and MIKE 21, covering a total river length of 889 km (726 km in 1D and 163 km in 2D).

Despite significant efforts in updating the FRMP, no river sectors identified during Cycle I were selected for remodeling in Cycle II by the National Administration "Romanian Waters" and the National Institute of Hydrology and Water Management for the Dobrogea-Litoral basin.

Against this backdrop, the PhD Thesis entitled "Digital Terrain Modeling for Flood Mitigation in Northern Dobrogea" focuses on delineating flood hazard boundaries for the localities Nistorești and Războieni, crossed by the Casimcea River—a watercourse designated as an APSFR (Area of Potential Significant Flood Risk) during Cycle I. The methodology integrates a high-resolution Digital Terrain Model (DTM) with 1D and 2D hydraulic modeling in HEC-RAS.

## **Research Findings**

## Flood Frequency Analysis

The flood frequency analysis conducted on maximum discharge data from the Casimcea basin showed that it is challenging to recommend a single optimal Probability Density Function (PDF) for all rivers studied. Further exploration of probability distributions tailored to arid and semi-arid regions is essential, especially since discharges derived from frequency analysis were lower than those listed in the Flood Prevention, Protection, and Mitigation Plan (PPPDEI).

Consequently, hydraulic modeling was based on PPPDEI discharges to avoid potential underestimation of flood risk.

## **Terrain Modeling**

The generation of a high-resolution DTM was achieved by integrating modern spatial data acquisition technologies, such as GNSS RTK systems, LiDAR technology, and aerial photogrammetry, complemented by precise ground surveys. Specialized software was used for processing, filtering, modeling, and validating the acquired data.

### **Hydraulic Modeling**

Flood mapping utilized HEC-RAS v6.7, developed by USACE, enabling both 1D and 2D hydraulic modeling, providing flexibility for simulating various hydraulic regimes and assessing flood extents.

## **Personal Contributions**

This work brings six major original contributions with strong practical and methodological significance:

- Integration of modern technologies for high-resolution DTM generation:
- Acquisition and processing of precise topographic data using GNSS RTK and UAS equipped with LiDAR and RGB cameras.

Personal execution of aerial missions: flight planning, sensor calibration, data collection, and integration into hydraulic modeling workflows, ensuring full control of data quality.

- Comparative evaluation of 1D and 2D hydraulic modeling:
- Detailed simulation of steady and unsteady flow regimes, using both constant and variable discharges for realistic flood scenarios.
- Highlighting the limitations of 1D modeling in complex geomorphological contexts and identifying conditions favoring stable results with steady discharges.

Application of 2D modeling for complex flood scenarios:

- Configuration and calibration of 2D simulations through mesh refinement and domain adjustments based on terrain characteristics.
- Internal validation of 2D models through correlation with ground-collected topographic data and empirical observations, ensuring robust numerical results.

Correlation of modeling outputs with official hazard maps:

- Comparative analysis between model-derived flood extents and FHRM from FRMP Cycles I and II.
- Identification of significant discrepancies in Nistorești and Războieni, caused by outdated hazard maps and generalized modeling methods lacking local calibration.
- Integration of frequency analysis into discharge validation to understand the impact of statistical distributions on flood extents.

Proposals to improve flood hazard assessment:

- 2D modeling results, corroborated by field observations, underscore the need to update flood boundaries in Nistorești and Războieni due to major mismatches with existing maps.
- Advocating for the reconstruction of historical flood events as an additional validation method for basins with incomplete or discontinuous data records.

Optimization of frequency analysis for arid regions:

- Development of a tailored methodology for frequency analysis in intermittent-flow catchments typical of Dobrogea.
- Testing and validation of theoretical distributions (Gamma, EV3-Min, Pareto, GEV-Min) using Kolmogorov-Smirnov and L-moment methods, complemented by error functions (RMSE, NSE, R<sup>2</sup>).

- Demonstrating that classical PDFs (e.g., Gumbel, Log-Normal) significantly overestimate extreme flows in low-probability scenarios, highlighting the need for locally adapted statistical models.
- Although statistically valid, frequency-derived flows were replaced by PPPDEI discharges in hydraulic modeling to ensure conservative and safety-oriented flood risk estimations.

## **Future Perspectives**

The findings of this study provide a robust framework for flood hazard assessment in small catchments and open pathways for future research:

## **Basin-scale flood modeling:**

• Extending 2D modeling to the entire Casimcea basin, incorporating tributaries and sub-basins, to simulate flood wave propagation and identify high-risk zones.

## **Integration of rainfall-runoff modeling:**

 Coupling hydraulic simulations with hydrological models capable of simulating runoff generation from precipitation, thus enabling flood scenario assessment under current climatic conditions.

#### Historical flood event validation:

• Correlating 2D models with documented flood events (e.g., 2002 flood) using satellite archives, local photographs, and community accounts for qualitative and quantitative model validation.

### Incorporating vulnerability and exposure analysis:

 Moving from hazard analysis to full risk assessment by integrating exposure data (population, infrastructure, socio-economic assets) with hydraulic outputs for emergency planning and risk management.

### Advancing frequency analysis with hybrid and Bayesian approaches:

• Implementing advanced statistical testing (e.g., modified Anderson-Darling, Bayesian methods) and hybrid frameworks combining empirical, historical, and simulated data to refine flow estimates for rare events (e.g., 0.1% probability floods) in arid regions.

## SELECTED BIBLIOGRAPHY

- [01] Aditya, F. Gusmayanti E. Sudrajat J. (2021) Rainfall trend analysis using Mann-Kendall and Sen's slope estimator test in West Kalimantan. *IOP Conference Series: Earth and Environmental Science, Volume 893*, 2nd International Conference on Tropical Meteorology and Atmospheric Sciences 23 25 March 2021, Jakarta, Indonesia
- [03] **Agenția Europeană de Mediu.** (2016) Flood risks and environmental vulnerability. Exploring the synergies between floodplain restoration, water policies and thematic policies. *EEA Raport 1/2016*.
- [04] **Agenția Europeană de Mediu.** (2017) Climate change, impacts and vulnerability in Europe 2016 An indicator-based report. *Publications Office*.
- [14] **Banca Mondială.** (2018) Romania Water Diagnostic Report. Moving toward EU Compliance, Inclusion, and Water Security.
- [16] **Banca Mondială.** (2020) Rezultatul 1: Inventariere și Plan de lucru din cadrul proiectului de Servicii de Asistență Tehnică Rambursabile privind "Asistență Tehnică pentru Elaborarea Planurilor de Management al Riscului la Inundații pentru România.
- [20] **Boyer, J.F.** (2002) Khronostat Software for Statistical Analysis of Time Series. *IRD UR2, Program 21 FRIEND AOC, UMRGBE Hydrology Team, University of Montpellier II, Paris Mines School.*
- [26] **Cerneagă, C., Dobrică, G., Maftei, C.** (2022) Hydraulic Modeling with HEC-RAS 2D in the Urban Area of Casimcea (Romania) Catchment. In: Chenchouni, H., et. al. New Prospects in Environmental Geosciences and Hydrogeosciences. CAJG 2019. Advances in Science, Technology & Innovation. Springer, Cham. <a href="https://link.springer.com/chapter/10.1007/978-3-030-72543-3">https://link.springer.com/chapter/10.1007/978-3-030-72543-3</a> 105
- [27] **Cerneagă, C. and Maftei, C.** (2021) Flood frequency analysis of Casimcea river. IOP Conference Series: Materials Science and Engineering. 1138. <a href="https://iopscience.iop.org/article/10.1088/1757-899X/1138/1/012014">https://iopscience.iop.org/article/10.1088/1757-899X/1138/1/012014</a>
- [29] Chendeş, V. Rădulescu, D. Rîndaşu, S. Ion, B. Achim, D. Preda, A. (2014) Aspecte metodologice privind realizarea hărților de risc la inundații raportate în cadrul Directivei 2007/60/EC. *Hidrotehnica*, 59.
- [33] **Comisia Europeană.** (2015) EU overview of methodologies used in preparation of Flood Hazard and Flood Risk Maps.
- [37] Curtea de Conturi a Uniunii Europene. (2018) Floods Directive: progress in assessing risks, while planning and implementation need to improve. *Special report no 25*.
- [42] **EXCIMAP**. (2007) Handbook on good practices for flood mapping in Europe. *EXCIMAP* (a European exchange circle on flood mapping) Endorsed by Water Directors, 29-30 November 2007.
- [43] Fatica, S. Kátay, G. Rancan, M. (2022) Floods and firms: vulnerabilities and resilience to natural disasters in Europe. *European Commission, Ispra, JRC132125*.

- [49] **Goswami, G., Prasad, R.K. & Kumar, D.** (2023) Hydrodynamic flood modeling of Dikrong River in Arunachal Pradesh, India: a simplified approach using HEC-RAS 6.1. *Model. Earth Syst. Environ.* 9, 331–345. https://doi.org/10.1007/s40808-022-01507-2
- [56] **Hosking J.R.M. Wallis J.R.** (1997) Regional Frequency Analysis An Approach Based on L-Moment. *Cambridge University Pres, Cambridge, UK*. http://dx.doi.org/10.1017/cbo9780511529443
- [58] **Ielenicz, M.** (2003) Relieful litostructural din podișul Dobrogei. Analele *Universității* "Valahia" Târgoviște, Seria Geografie, Tomul 3.
- [59] **Inspectoratul General pentru Situații de Urgență.** (2016) Country report 5.1 Conditionality Romania. *Condiționalitate Ex-ante 2013-2020*.
- [61] **Iordan, D.** (2014) Aplicarea tehnologiilor laser la studiul topografic al bazinului hidrografic Someș-Tisa. *Universitatea din București, Facultatea de Geologie și Geofizică*.
- [69] Land Professional Group of RICS (2010) Guidelines for the use of GNSS in land surveying and mapping. 2nd edition, guidance note. UK.
- [73] **Maftei, C. Papatheodorou, K.** (2015) Flash Flood Prone Area Assessment Using Geomorphological and Hydraulic Model. *J. Environ. Prot. Ecol.* pp 16, 63–73.
- [74] **Maftei, C. Papatheodorou, K.** (2016) Mathematical Models Used for Hydrological Floodplain Modeling. In Extreme Weather and Impacts of Climate Change on Water Resources in the Dobrogea Region. *IGI Global: Hershey, PA, USA*, pp 69–100.
- [75] **Maftei, C. Cerneagă, C. Vaseashta, A.** (2025) Predictive Modeling of Flood Frequency Utilizing Analysis of Casimcea River in Romania. Hydrology (ISSN 2306-5338). Basel, June 2025. <a href="https://www.mdpi.com/2306-5338/12/7/172">https://www.mdpi.com/2306-5338/12/7/172</a>
- [77] **Merz, R. Blöschl, G.** (2005) Flood frequency regionalisation Spatial proximity vs. catchment attributes. *Journal of Hydrology*, 302(1–4), 283–306. https://doi.org/10.1016/j.jhydrol.2004.07.018
- [78] Meylan, P. Musy, A. (1999) Hydrologie frequentielle. \*H\*G\*A\*, Bucharest.
- [79] **Meylan, P. Favre, A.C. Musy, A.** (2011) Predictive hydrology: a frequency analysis approach. *CRC Press*.
- [84] **Organizația Mondială de Meteorologie.** (2012) Management of Flash Floods A Tool for Integrated Flood Management.
- [85] **Organizația Mondială de Meteorologie.** (2022) Assessment Guidelines for End-to-End Flood Forecasting and Early Warning System.
- [87] **Parlamentul European și Consiliul Uniunii Europene.** (2007) Directiva 2007/60/CE privind evaluarea și gestionarea riscurilor de inundații.
- [90] **Pike, R.J. Evans, I.S. Hengl, T.** (2009) Chapter 1 Geomorphometry: A Brief Guide. *Developments in Soil Science*. Volume 33, pp 3-30.
- [92] **Programul Global pentru Reducerea Riscurilor de Dezastre.** (2016) Country Risk Profiles for Floods and Earthquakes.

- [97] **Seghedi, A. Oaie, Gh. Anițăi, N.** (2018) Dobrogea patrimoniu geologic. *GeoEcoMar, București*.
- [103] **Török-Oance**, **M.** (2001) Aplicații Ale Sig În Geomorfologie (I). Realizarea Modelului Numeric Al Terenului Şi Calcularea Unor Elemente De Morfometrie. *Analele Universității de Vest din Timișoara*, *GEOGRAFIE*, vol. XI-XII, 2001-2002, pp. 17-30
- [106] **Vaduva**, **R.** (2014) Planificarea Integrată a Teritoriului în Condiții de Incertitudine a Riscului la Inundații. *Universitatea Politehnica Timișoara*.
- [110] **Broșura Planurile de Management al Riscului la Inundații.** (2022). *Broșuri RO FLOODS* versiunea mai 2022
- [114] **Planul de Management al Riscului la Inundații,** Administrația Bazinală de Apă Dobrogea Litoral 2016
- [115] **Planul de Management al Riscului la Inundații** Ciclul II Sinteza Națională perioada 2023 2027.
- [116] **Planul de Management al Riscului la Inundații** la nivelul Administrației Bazinale de Apă Dobrogea Litoral aferent Ciclului II de implementare a Directivei Inundații perioada 2023 2027.